Mitigating antibiotic pollution using cyanobacteria: removal efficiency, pathways and metabolism

Minmin Pan[a,b,c], Tao Lyu*[,d], Lumeng Zhan[a,b], Victor Matamoros[e], Irini Angelidaki[c], Mick Cooper[f], Kai Tang [c], Gang Pan*[,a,b,f]

[a]*Research Center for Eco-Environmental Sciences, Chinese Academy of Sciences, Beijing 100085, China*

[b]*Sino-Danish College of University of Chinese Academy of Sciences, Beijing 100049, China*

[c]*Department of Environmental Engineering, Technical University of Denmark, DK-2899 Lyngby, Denmark*

[d]*Cranfield Water Science Institute, Cranfield University, College Road, Cranfield, Bedfordshire MK43 0AL, UK*

[e]*Department of Environmental Chemistry, IDAEA-CSIC, Jordi Girona, 18-26, E-08034 Barcelona, Spain*

[f]*School of Animal, Rural and Environmental Sciences, Nottingham Trent University, Brackenhurst Campus, NG25 0QF, UK*

**Corresponding authors*: gang.pan@ntu.ac.uk (G. Pan); t.lyu@cranfield.ac.uk (T. Lyu).

ABSTRACT

The occurrence of pharmaceuticals and personal care products (PPCPs) in wastewater poses huge environmental threats, even at trace concentrations, and novel approaches are urged due to the inefficiencies of conventional wastewater treatment plants, especially when processing contaminants at high concentrations. Meanwhile, another widespread problem in the aquatic domain is the occurrence of harmful algal blooms (HABs) which cause serious damage to the ecosystem, but have rarely been investigated for possible valorization. This study investigated the possibilities, mechanisms, and

effects of toxin release of using a harmful cyanobacterial species, *Microcystis aeruginosa* (*M. aeruginosa*), in order to remove the widely used drug, tetracycline, at high concentration. The results were compared with the performance obtained by the use of the hitherto generally-selected chlorophyte alga *Chlorella pyrenoidosa* (*C. pyrenoidosa*) for tetracycline concentrations of 10-100 mg L^{-1}. *M. aeruginosa* exhibited a much more effective and rapid tetracycline removal (over 98.0% removal in 2 days) than did *C. pyrenoidosa* (36.7%-93.9% in 2 days). A comprehensive kinetic investigation into probable removal pathways indicated that, theoretically, bio-remediation dominated the process by *M. aeruginosa* (71.6%), while only accounting for 20.5% by *C. pyrenoidosa*. Both microalgae promoted the hydrolysis of tetracycline under conditions of increased pH and inhibited abiotic photolytic reactions by the shading effect to the water column, when compared with control experiments. Although identical degradation by-products were identified from treatments by both microalgal species, distinct by-products were also confirmed, unique to each treatment. Moreover, the growth of *M. aeruginosa* biomass exhibited strong tolerance to tetracycline exposure and released significantly lower levels of microcystin-LR, compared with the control systems. This study supports the possibility of reusing HABs species for the effective remediation of antibiotics at high concentrations. We have further suggested possible mechanisms for remediation and demonstrated control of toxin release.

Keywords: Harmful Algal Blooms (HABs), Microalgae, Micropollutants, Microcystin control, PPCPs.

1. Introduction

Pharmaceuticals and personal care products (PPCPs) have been extensively detected in aquatic systems, and pose serious hazards to human health and ecology even at trace levels (Suárez et al., 2008). The global consumption of antibiotics alone has been estimated at 100-200k tons (Qian et al., 2012), however, 25%-75% of the consumed antibiotics are excreted from living systems and contaminate natural waters (Sarmah et al., 2006). Such antibiotics are barely removed in conventional wastewater treatment plants (WWTPs) due to their antibacterial properties (Wang et al., 2013). Tetracycline (Fig. S1.) is the second most widely-used antibiotic, often employed for the treatment of many different bacterial infections as diverse as severe acne, food poisoning, and sexually transmitted diseases. The presence of residual tetracycline at trace levels in the environment as a whole might lead to further development of antibiotic-resistant bacteria, which, in turn, would be a major health problem. Worse still, tetracycline exposure at high concentrations generates the equally serious environmental problem of acute toxicity to the aquatic and edaphic organisms (Daghrir and Drogui, 2013). To date, more attention has been paid to the investigation of tetracycline removal at low concentrations, e.g. μg/L (Kim et al., 2005), however, tetracycline could be present at levels up to 200 mg L^{-1} in pharmaceutical wastewater (Song et al., 2019). The acute toxicity effect from such high concentrations of tetracycline raises significant challenges to conventional wastewater treatment methods. Previous studies have indicated that WWTPs can only achieve up to 30% removal of this drug (Watkinson et al., 2009), which may be attributed to the toxic effects of tetracycline on the bacterial population present in aerobic sludge (Halling-Sørensen, 2001), especially with exposure at high concentration. Thus, development of technology

for the effective and economic mitigation of tetracycline at high concentrations is urgently required.

Various approaches, such as flocculation (Fu et al., 2015), advanced oxidation (Hou et al., 2016), and adsorption (Gao et al., 2012), have been proven to effectively remove tetracycline from wastewater at high concentrations. However, such methods require increasing dosage of additional chemicals with rising concentration of tetracycline. Consequently, the large scale application of such techniques is still hindered by their relatively high costs and the potential problem of secondary pollutants (Tang et al., 2016). Microalgal technology has been recognised as an eco-friendly, and cost-effective method for water treatment, including removal of emerging contaminants (Matamoros et al., 2016). A further advantage of this technique is the potential reuse of the algal biomass (Pan et al., 2018). Therefore, microalgal species with high economic value, such as *Chlorella pyrenoidosa* (*C. pyrenoidosa*; Sun et al., 2011), have hitherto been mostly selected for wastewater treatment. Cyanobacteria, although the most well-known species responsible for harmful algal blooms (HABs) in eutrophic waters (Zhang et al., 2018), is often neglected because of the production of toxic microcystins as by-products of metabolism (Hitzfeld et al., 2000). From the perspective of wastewater treatment, its characteristics of rapid growth, high nutrient uptake capability, and low requirement for a favourable environment (e.g. temperature and pH), could make cyanobacteria an ideal microalgae species, if the release of unwanted toxins could be controlled during the process (Rzymski et al., 2014).

Microalgal technology has been demonstrated to effectively remove tetracycline under low initial concentration levels (<2 mg L^{-1}) (Norvill et al., 2017; de Godos et al., 2012). However, studies on microalgal technology for the treatment of wastewater containing high concentrations of tetracycline, have been rarely investigated.

Furthermore, some microalgal species exhibit a Gram-negative-bacteria-like prokaryotic structure, in which cases tetracycline could generate biphasic hormetic effects, *i.e.* inhibition at high doses and stimulation at low doses (Wan et al., 2015). Thus, a high initial concentration of the drug may lead to a dramatically low removal performance, an effect which has rarely been thoroughly investigated. Therefore, research on the removal, by microalgae, of high concentrations of tetracycline from PPCPs-polluted wastewater is needed and is still challenging.

Considering the application of different microalgal species, full-scale microalgae treatment systems, *e.g.*, tubular photo-bioreactor and raceway ponds, have been successfully applied for the treatment of various wastewaters, such as municipal wastewater (Rawat et al., 2011) and livestock effluent (Wang et al., 2016). Nevertheless, the major concern of using cyanobacteria to replace other commonly-used microalgae species, *e.g.*, *C. pyrenoidosa*, is the potential risk of toxin release during algal death and cell lysis (Paerl and Otten, 2013). A previous study has demonstrated the significant decrease of microcystin production and release from cyanobacteria on exposure to tetracycline up to 10 mg L^{-1} (Ye et al., 2017). This effect may have been due to the blocking of peptide synthesis, controlling the production of microcystin-LR (Ye et al., 2017) and a corresponding enhancement in the production of reactive oxygen species (ROS) (Yang et al., 2013) due to the presence of tetracycline. However, release of toxins from cyanobacteria under higher tetracycline concentrations (>10 mg L^{-1}) has rarely been investigated. Release of toxins from cyanobacteria mainly occurs during algal death and cell lysis. Thus, the monitoring of algal cell vitality and the measurement of toxin production during the process is essential in order to evaluate the safety envelope of the treatment technology.

The mechanisms of antibiotics removal, including pathways and metabolism, by different microalgal species, always vary. It is generally agreed that comprehensive pathways, i.e. photolysis, hydrolysis, cation-binding, adsorption, bioaccumulation and biodegradation, may simultaneously contribute to the removal of antibiotics from the environment (Xiong et al., 2017a). It has been found that photodegradation mainly contributed to tetracycline removal (Norvill et al., 2017), however, de Godos *et al*. (2012) reported that biosorption and photodegradation are both predominant pathways for tetracycline removal during treatment by different microalgae. Thus, quantitative investigation of removal pathways is vitally important for the understanding of cyanobacteria-based treatment of tetracycline. Moreover, Halling-Sørensen *et al*. (2002) have highlighted that anhydrotetracycline (ATC) and 4-epianhydrotetracycline (EATC) could be major by-products of metabolism, and which may be more toxic than the parent compound, during remediation in aqueous conditions (Halling-Sørensen et al., 2002). Thus, identification of the by-products of degradation is also important in order to systematically understand remediation mechanisms (Halling-Sørensen et al., 2002) and potential environmental impacts.

In this study, we investigated the potential use of harmful cyanobacteria to effectively and safely remediate wastewater containing high concentration of tetracycline, and elucidated the probable mechanisms of removal. The removal efficiencies of tetracycline by the cyanobacteria, *Microcystis aeruginosa* (*M. aeruginosa*), were compared with the treatment by representative wastewater treatment microalgal species *C. pyrenoidosa* at relatively high initial concentrations (10-100 mg L^{-1}) of the drug. Different pathways and degradation by-products of tetracycline aided the elucidation of likely removal mechanisms. Algal biomass growth and cell vitality were characterised to estimate possibilities for biomass reuse. Moreover, levels of toxic

147 microcystin-LR, released from *M. aeruginosa*, was monitored, in order to assess water
148 reuse/discharge safety.

149 2. Materials and methods

150 *2.1 Materials*

151 Two species of microalgae strains, *M. aeruginosa* and *C. pyrenoidosa*, were
152 purchased from the freshwater algae culture collection at the Institute of Hydrobiology
153 (FACHB), Wuhan, China, and cultivated in BG11 media (Table S1) prior use.
154 Tetracycline was obtained from J&K Scientific Ltd., Beijing, China. Microcystin-LR
155 standard (SB05-287-2012) was purchased from the National Standard Material Center
156 of China (Beijing, China). All reagents used were of analytical grade and ultrapure
157 water (18 MΩ·cm) was used in all experiments.

158 *2.2 Experimental operation*

159 The removal performance of tetracycline by the two microalgal species was
160 evaluated under different initial tetracycline concentrations. An appropriate volume of a
161 tetracycline solution in ultra-pure water was added into each BG11 culture medium,
162 resulting in three different concentrations of 10, 50, and 100 mg L^{-1}. Three control
163 groups were set up to elucidate the removal of tetracycline by natural degradation
164 (photolysis and hydrolysis) and binding to divalent cations (calcium, magnesium, cobalt)
165 present in the BG11 culture media. The groups comprised 1) BG11 medium with
166 tetracycline, but without microalgae under irradiation, was set as a *light control*, 2)
167 BG11 medium with tetracycline, but without microalgae and irradiation, was set as a
168 *dark control*, and 3) pure water with tetracycline, but without microalgae and irradiation,
169 was set as a *chemical control*. ~~To clarify the removal of tetracycline by natural~~
170 ~~degradation (photolysis and hydrolysis) and binding to divalent cations (calcium,~~

~~magnesium, cobalt) present in the BG11 culture medium, a culture medium with tetracycline but without microalgae was set as the light control, whereas a sample of BG11 culture media with microalgae, but without tetracycline addition, was set as the microalgal control.~~ Media with microalgae addition are hitherto referred to as *treatment groups*.

The treatments were conducted in Erlenmeyer flasks (1L) with 500 mL working volume. Different microalgae species have distinct cell sizes and growth rates, therefore, previous studies usually conducted wastewater treatment experiments under similar initial algal biomass concentrations in order to allow the results to be directly comparable (Arbib et al., 2014). To better compare the tetracycline removal performance, the two species were separately pre-cultured until the late exponential phase. Afterwards, both microalgal species were inoculated into corresponding flasks to achieve an identical optical density (OD680) of 0.103 ± 0.016, which represented the same biomass concentrations (7.12 x 10^6 cell mL^{-1} *M. aeruginosa* and 7.50 x 10^5 cell mL^{-1} *C. pyrenoidosa*). All flasks were placed in an incubator maintained at 28±1 ^oC and illuminated by white light (full-spectrum white LED; Ledvance GmbH, Garching, Germany; intensity 1600 lux; light:dark ratio of 12:12h). All flasks were swirled manually three times (5 mins each) each day. The experimental setup with the initial tetracycline concentration of 50 mg L^{-1} was selected for comprehensive study into the possible removal pathways. ~~In addition, a dark control group (flasks wrapped in aluminium foil), which contained only tetracycline in growth media without algae, was prepared in order to determine abiotic hydrolysis and cation binding of tetracycline.~~ Each group was set up in triplicate and operated for 13 days. In total, 36 treatments were conducted for the investigation.

2.3 Sampling and analysis

196 *2.3.1 Sampling*

197 The pH of each treatment suspension was measured daily directly in the flask
198 using a PHB-600R pH meter (Omega Engineering, Norwalk, USA). In addition,
199 samples (0.2 mL) were taken daily for algal cell counting, while another sample (2 mL)
200 was taken from each flask at 0, 2, 4, 6, 16 and 24 hours, and then daily until day 13, for
201 determination of tetracycline concentration, by ultrahigh-performance liquid
202 chromatography (Waters Acquity UPLC, Waters Corp., Milford, USA) as described
203 later. Samples for investigation into possible tetracycline removal pathways,
204 microcystin-LR production, and detection of degradation by-products, were also taken
205 on the corresponding days.

206 *2.3.2 Tetracycline analysis and removal pathways*

207 Thus, tetracycline removal kinetics by natural hydrolysis, photolysis, and cation-
208 binding were determined by sampling at hour 0, 2, 4, 10, 16, and daily from day 1 to
209 day 11. The chemical control group could be categorised as the abiotic hydrolysis of
210 tetracycline. The difference between tetracycline removal in the dark and in the
211 chemical control groups was considered to represent tetracycline removal caused by
212 cation-binding. Meanwhile, differences between tetracycline removal in light and dark
213 control groups enabled estimation of abiotic photolysis process. The sampling methods
214 for tetracycline distribution (in water, via bio-adsorption, and via bio--accumulation) are
215 described in Text S1.1. ~~The light control theoretically enable estimation of tetracycline~~
216 ~~removal through photolysis, hydrolysis, and cation-binding processes. Meanwhile, the~~
217 ~~dark control was conducted to simulate the theoretical tetracycline removal through~~
218 ~~hydrolysis and cation-binding processes. Each 2 mL water sample was centrifuged~~
219 ~~(4500 rpm for 15 min) in order to separate the algae and supernatant, with the latter~~
220 ~~being subsequently used for the determination of tetracycline concentration remaining~~

~~in water. The sample was further passed through a membrane filter (0.22 μm) prior to injection into the UPLC. Notably, at 24, 240 and 312 hours, additional samples (5 mL) were taken from the flasks and centrifuged as described previously. After complete re-suspension and homogenization with ultrapure water (5 mL), each algal pellet was washed and re-centrifuged, the supernatant being analysed for bio-adsorbed tetracycline. The algal pellet was then homogenized into a methanol and dichloromethane mixture (5 mL; 2:1, v/v). After further treatment by freeze-thawing with liquid nitrogen (x3), samples were centrifuged and the supernatant quantified as the intracellular bioaccumulated tetracycline fraction.~~ The analysis parameters for UV detection of tetracycline by Acquity UPLC-PDA (Diode Array Detector) are detailed in S1.1.

2.3.3 Detection of degradation by-products

Filtered water samples (supernatant phase, 0.22 μm membrane filter), from treatments spiked with an initial tetracycline concentration of 50 mg L^{-1}, were used to identify tetracycline degradation by-products by analysis with an Acquity UPLC coupled with a Waters Xevo G2 ToF-MS detector (Waters Corp., Milford, USA). Only samples collected at 24 and 312 hours were processed. The working parameters for the Acquity UPLC are described in the supporting information (Text S1. 2) and the working parameters of the ToF-MS were: mass range 50-1200 Da, scan time 1.5 sec, collision energy 6V, collision energy ramp 15 to 30 V, cone voltage 40 V, positive polarity.

2.3.4 Microcystin-LR measurement

The most toxic microcystin compound, microcystin-LR, was detected by UPLC-UV in both intracellular and extracellular fractions in the samples collected at 10, 60 and 240 hours from the treatment groups with an initial tetracycline concentration of 50 mg L^{-1}. Specifically, 50 mL sample was initially centrifuged (4800 rpm for 15 min). The supernatant thus produced was then used for the quantification of released

246 microcystin-LR after pre-concentration by SPE (Oasis R MCX 6cc, 500mg, Waters
247 Corp., Milford, USA). The SPE was initially activated with 100% methanol (10 mL),
248 followed by a wash-out of ultrapure water (20 mL, 3 mL min^{-1}). A gradient
249 concentration of methanol (0-20%, v/v) was utilized for the wash-out of impurities and
250 methanol (3 ml, 35% v/v) for elution of the microcystin-LR. After collection, the eluent
251 was evaporated under dry nitrogen to 1.2 mL.

252 The algal pellet was also analysed for intracellular microcystin-LR. Briefly, after
253 washing three times with ultrapure water, the pellet was dissolved with methanol (80%
254 v/v) and freeze-thawing with liquid nitrogen (x3) in order to fragment the algal cells,
255 and to extract the microcystin-LR. Finally, 1 mL sample was concentrated by
256 evaporation under dry nitrogen at room temperature. The working parameters of
257 Acquity UPLC for microcystin-LR detection are described in S.1.3.

258 *2.4 Microalgal growth monitoring*

259 Cell densities of both microalgae species were monitored daily using a
260 hemocytometer. After sampling on day 1, 3, 6, and 10, cell pigments were detected and
261 calculated as described in S1.4.

262 *2.5 Calculation and statistical analysis*

263 The Pseudo-first-order kinetic model (1) was used to simulate the removal,
264 desorption and decline of accumulated tetracycline:~~degradation removal, adsorption and~~
265 ~~accumulation of tetracycline based on equation (1) and (2):~~

266 $$\ln(C_0/C) = k \times t \quad (1)$$

267 Meanwhile, according to (Choi et al., 2020), the concentration changes
268 through adsorption and accumulation by microalgae was simulated with modified
269 pseudo-first-order kinetic model (2):

$$\ln(1-C_0/C) = -k \times t \quad (2)$$

where, C_0 is the concentration of tetracycline at time t=0 and C is the tetracycline at time t=t; k represents the pseudo-first-order kinetic rate constant; t is the time.

SPSS 19.0 (IBM Corporation, Armonk, USA) and Origin 8.5 (OriginLab, Northampton, USA) were used to analyse and to plot the data, respectively. One-way ANOVA and Tukey's multiple comparison test were used to compare ($p<0.05$) water quality parameters between different treatment systems at each sampling point.

3. Results and Discussion

3.1 Tetracycline removal efficiency and kinetics

Tetracycline is a chemically reactive compound which can be degraded through photolysis and/or hydrolysis processes (Yi et al., 2016; Jiao et al., 2008). This characteristic supports the observation that the tetracycline degraded in all control groups, even without addition of microalgae. In this study, *C. pyrenoidosa* was selected as a representative, widely-investigated, and safe microalgal species for wastewater treatment (Sun et al., 2011). The comparison of tetracycline removal efficiencies between *M. aeruginosa* and *C. pyrenoidosa* could contribute to a better understanding of the advantages or drawbacks for treatment of wastewater, containing high concentrations of tetracycline, by the newly proposed HABs species over conventional microalgae species. For *C. pyrenoidosa* treatments (Fig. 1a), from an initial concentration of 10 mg L^{-1}, the tetracycline concentration significantly decreased to 0.65 mg L^{-1} (93.9% removal) by day 2 and then reached 0.01 mg L^{-1} (99% removal) on day 11. However, the *M. aeruginosa* treatments showed a much faster removal rate, and achieved 0.01 mg L^{-1} (99% removal) at day 2 which was furthermore maintained until day 11 (Fig. 1a). Previous studies have indicated that higher tetracycline concentration

might hinder microalgae growth (Ye et al., 2017) and therefore affect drug removal. This observation is supported in this study by the *C. pyrenoidosa* groups, at the higher initial concentration of 50 mg L^{-1} (Fig. 1b), where tetracycline concentrations decreased faster than those in the control group, until day 4 after which it maintained at 0.7 mg L^{-1} (98.6% removal rate) and performed similarly to the control. The growth of the algal biomass may act to decrease the light penetration in the water and thus affect photolysis and/or hydrolysis removal of tetracycline. Thus, at the initial concentration of 100 mg L^{-1}, the tetracycline removal in *C. pyrenoidosa* groups became similar, or even less effective, when compared to the control (Fig. 1c).

The *M. aeruginosa* groups consistently exhibited significantly superior performance for tetracycline removal at high initial concentrations of 50 and 100 mg L^{-1}, where the similar tendencies of rapid removal over 98.0% were achieved within 1 and 2 days, respectively (Fig. 1b and c). *M. aeruginosa,* as a typical cyanobacterial alga, demonstrated a rapid reproduction rate, which, however, could lead to the appearance of serious harmful algal blooms within several days in eutrophic lakes (Paerl and Otten, 2013). The existence of *M. aeruginosa* has been observed worldwide, regardless of temperature and pH variance of the water (Paerl and Otten, 2013), which may indicate its high tolerance against any antibiotic effects. The results demonstrated that the harmful cyanobacteria, *M. aeruginosa*, could rapidly and effectively remove tetracycline within limitations of initial concentration. Previous studies indicated that, in algal ponds, only 69±1% tetracycline was removed from an initial concentration of 2 mg L^{-1} (de Godos et al., 2012), and 93% tetracycline was eliminated from an initial concentration of 0.1 mg L^{-1} in 4 days (Norvill et al., 2017). Comparatively, the *M. aeruginosa* demonstrated a much higher and faster removal capacity of tetracycline over a wide range of initial concentrations, up to 100 mg L^{-1}.

Tetracycline removal is widely indicated by studies to follow the pseudo-first-order kinetics in high-rate algal pond (HRAP) systems (de Godos et al., 2012, Norvill et al., 2017). The results of tetracycline removal in this study also exhibited good correspondence with the pseudo-first-order kinetic model (Fig. 1, Table 1, $R^2>0.94$). Generally, elevation of levels of tetracycline significantly decreased the removal rates (k). ~~Meanwhile, the light controls (including photolysis, hydrolysis and cation-binding processes) achieved 1.7 times higher k value than did the dark controls (including hydrolysis and cation-binding processes), indicating the significance of photolysis to tetracycline removal.~~ Except for the *C. pyrenoidosa* with 100 mg L^{-1} tetracycline, in which the growth of microalgae probably inhibited the photolysis of tetracycline and generated lower removal rates than the control, all other groups of both microalgae species achieved greater removal rates than the control. This indicated a significant promotion of the presence of microalgae on tetracycline removal than the natural removal processes contributed by hydrolysis, photolysis, and cation-binding, especially with *M. aeruginosa* (5.1-12.1 times higher than the control). The results further demonstrated that, overall, *M. aeruginosa* exhibited significantly higher removal rates, at all tetracycline levels, than did the *C. pyrenoidosa* ($p<0.05$), indicating a better general tetracycline removal ability of *M. aeruginosa* than the *C. pyrenoidosa*. Compared with previous studies, the pseudo-first-order kinetic rate results also showed statistically better tetracycline removal kinetic achieved by *M.aeruginosa* (0.17-0.077, 10-100 mg L^{-1} tetracycline) than that achieved by the HRAP (0.091-0.038, 0-88 mg TSS L^{-1} biomass, 2 mg L^{-1} tetracycline; (de Godos et al., 2012) and photolysis/hydrolysis processes (0.0014-0.0065, 20-100 mg L^{-1} tetracycline; Yi et al., 2016; Jiao et al., 2008).

3.2 Tetracycline removal pathways

The experiment at the initial tetracycline concentration of 50 mg L^{-1} was further explored in order to understand the contributions from each pathway of removal. Considering the abiotic removal of tetracycline, processes of cation-binding, photolysis, and hydrolysis all contributed to the removal of tetracycline, acting however, at different levels (Fig. 2a-b, and S2a-b). The results from the chemical control group indicated that divalent cations present in the BG11 medium (Table S1), such as calcium, magnesium, and cobalt, could bind with tetracycline to form low solubility complexes (Pala-Ozkok et al., 2019), which contributed to a relatively constant tetracycline removal in the range of 1.42-4.08 mg L^{-1} (2.8-8.0%, Fig. S2a). Meanwhile, abiotic photolysis achieved a significant higher ($p<0.05$) removal rate ($k=0.029$) than did abiotic hydrolysis ($k=0.0069$, Table S2).

Results further indicated that the significantly higher removal rates of tetracycline ($p<0.05$) achieved by microalgae (especially by *M. aeruginosa*) ~~may be~~could be contributed through bioadsorption, bioaccumulation and biodegradation processes ~~of microalgae~~(Fig. 2c-d and S2c). ~~, but also by the impact of microalgal growth on abiotic hydrolytic and photolytic processes. Thus, tetracycline removal in the dark control groups was attributed to hydrolysis and cation-binding reactions (without microalgal influence). Moreover, the concentration difference between the light control groups and the dark control groups could be recognised as the theoretical removal by photolysis (without microalgal influence). From the control groups, it can be concluded that all abiotic photolysis, abiotic hydrolysis and cation-binding clearly contributed to tetracycline removal (Fig. 2a and b). Throughout the whole experiment,~~Simultaneous with the decline in concentration of tetracyclines in water, concentrations adsorbed and accumulated by both microalgae increased to a peak (uptake stage) inside one (*M. aeruginosa*) or two (*C. pyrenoidosa*) days. For the *C. pyrenoidosa* treatment groups, the

bioremediation (including bio-adsorption, bio-accumulation, and bio-degradation) contribution of the algae was always observed to be lower (<10.41 mg L^{-1}, less than 20.5% contribution) than those from abiotic photolysis, hydrolysis, and cation-binding. However, *M. aeruginosa* could be considered more effective for tetracycline bioremediation (39.02 mg L^{-1}, 71.6% contribution) providing a total removal efficiency of 98% after only 24 hours (Fig. 1, 2a and b). ~~Specifically, for bioremediation, the distribution results of residual tetracycline indicated that rapid adsorption (0.84 mg L-1 by M. aeruginosa and 2.46 mg L-1 by C. pyrenoidosa) and bioaccumulation (0.23 mg L-1 by M. aeruginosa and 5.56 mg L-1 by C. pyrenoidosa) of tetracycline could be achieved from day 1 by both microalgal species (Fig. 2c and d).~~ Previous studies also illustrated that tetracycline, owing to its hydrophilic nature, could be absorbed by the algal cell (de Godos et al., 2012). The compound has also been found to translocate into an algal cell through water and nutrient uptake pathways (Xiong et al., 2017a). However, the amount of tetracycline existing on cell surfaces (bioadsorption) and intracellular regions (bio-accumulation) in *M. aeruginosa* (1.07 mg L^{-1}, 2%) was much lower than that in *C. pyrenoidosa* (8.02 mg L^{-1}, 16%) on day 1. Afterwards, a gradual decline ofconcentrations from the peak was followed until day 13 (through eithermetabolization or release). Both concentrations of bioadsorbed and bioaccumulated tetracycline changed as a consequence of microalgal uptake and translocation, and could be well described by the pseudo-first-order kinetic model ($R2 \geq 0.90$, Table S2). Generally, in the uptake stage of tetracycline, the rates of bio-adsorption by both microalgal species were significantly higher than those of bio-accumulation ($p<0.05$) and, overall, *M. aeruginosa* achieved higher rates of bio-adsorption and bio-accumulation (k=0.66 and 0.19, respectively) than did *C. pyrenoidosa* (k=0.37 and 0.12, respectively, Table S2). Nevertheless, *M. aeruginosa* promoted a shorter uptake stage of tetracycline when

compared to *C. pyrenoidosa*. In the declining stage of tetracycline, the desorption rates of *M. aeruginosa* (k=0.23) were still significantly higher than that of *C. pyrenoidosa* (k=0.071), however, both species achieved similar decrease rates of accumulated tetracycline (k=0.012 and 0.011, respectively, p>0.05). Considering the superior tetracycline removal efficiency in *M. aeruginosa* treatment groups, the species presented significantly higher tetracycline biodegradation either inside the algal cell or by side effects outside the algal cell, when compared with *C. pyrenoidosa.*

Although the contributions of each pathway may vary, the results supported the hypothesis that all possible pathways, such as hydrolysis (tetracycline molecule split by chemically-catalysed addition of water), photolysis (light-activated oxidation), cation-binding (tetracycline binding with divalent cations), biodegradation (decomposition of tetracycline by microbial activity), bioadsorption (tetracycline passively concentrating and binding onto microalgal cells) and bioaccumulation (accumulation of tetracycline in the microalgae cells) (Yi et al., 2016; Jiao et al., 2008; Xiong et al., 2017b), have an effect on tetracycline removal. It should be noted that among the confirmed pathways, more than one mechanism can take place simultaneously and thus can influence each other. For example, the growth of microalgal biomass could reduce the intensity of light inside the water column and thus reduce tetracycline degradation by photolysis (de Godos et al., 2012) (Fig. 1c). Consequently, the realistic photolysis kinetics of tetracycline removal in both microalgal systems should be less than those of the theoretical results (Fig. 2~~ a and b~~c). Oppositely, it was observed that the inoculum and growth of both *M. aeruginosa* and *C. pyrenoidosa* led to an increase in solution pH than the controls. Moreover, the *M. aeruginosa* samples generally produced significantly higher pH levels than did the *C. pyrenoidosa* groups ($p<0.05$, Fig. S3). Previous studies have suggested a reduction in tetracycline hydrolysis half-life time by 2.68-3.27 -fold

418 with an increase of pH from 5 to 11 (22-25℃) (Yi et al., 2016). Thus, the realistic
419 hydrolysis of tetracycline under both microalgal treatments should be significantly
420 increased, above those theoretical hydrolysis kinetics (Fig. 2c~~2 a and b~~). The higher
421 levels of pH in the *M. aeruginosa* groups could promote a higher tetracycline hydrolysis
422 compared to that from the *C. pyrenoidosa* groups. Additionally, the elevated
423 photosynthetic processes occurring in microalgal treatments (Fig. ~~S5~~ S4 and ~~S6~~S5) may
424 increase both dissolved oxygen (DO) and pH, increasing the number of reactive oxygen
425 species (ROS) (Norvill et al., 2017), which, in turn, may also lead to the degradation of
426 tetracycline. ~~Moreover, the existence of microalgae and transition metals may lead to~~
427 ~~more complex tetracycline removal pathways such as indirect oxidation induced by~~
428 ~~microalgae secretions (Tian et al., 2019), photo-catalysis of transition metals (Wei et al.,~~
429 ~~2020), and affect the hydrolysis as well as the photolysis. Further investigations into the~~
430 ~~specific contributions of each tetracycline removal pathway and simulation of their~~
431 ~~potential kinetics should be carried out in order to gain understanding into the~~
432 ~~underlying mechanisms and thus help realize the implications.~~

433 *3.3 Tetracycline degradation by-products*

434 Water samples from both microalgal treatment groups were analysed by HPLC-
435 ToF-MS in order to determine potential degradation by-products and removal pathways.
436 Based on the results from the LC-ToF-MS analysis (Fig. ~~S3~~ S6 and ~~S4~~S7) and a review
437 of extant literature, we have elucidated that both microalgal systems utilised a common
438 degradation pathway (named PI), but also used additional specific pathways unique to
439 each species.

440 The results indicated that the tetracycline degradation process proceeded mainly
441 by two reaction patterns, *i.e.* changes to functional groups (gain and loss), and ring-
442 opening reactions (Cao et al., 2016). Relevant structures and ESI-ToFMS spectra are

illustrated in Fig. S7. By-product 1 (m/z 415) was detected in the samples (Fig. 3, PI), which indicated the removal of the N-methyl and C3 hydroxyl groups (Shen et al., 2020). Further loss of the C6 hydroxyl group and the formation of a conjugated double bond at C6-C5a position, resulted in the formation of by-product 2 (m/z 397) (Huang et al., 2019). This molecule could be further degraded via loss of the amide group at position C2 (Huang et al., 2019) and further demethylation of the secondary amine at position C4 (Guo et al., 2018), forming by-product 3 (m/z 340). The ring-opening reaction across C2 and C4a could lead to the formation of by-product 4 (m/z 284) (Huang et al., 2019), while further ring fragmentation across C5a and C11a with concurrent hydration could generate by-product 5 (m/z 183) (Zhou et al., 2020). Notably, most by-products of the PI pathway (m/z 415, 397, 340, 284) were also found in a tetracycline photo-catalysis degradation process mediated by a Bi_2WO_6-based material (Shen et al., 2020; Huang et al., 2019). Meanwhile, the final product from PI (m/z 183) was reported from an activated hydrogen peroxide oxidation process for tetracycline degradation (Zhou et al., 2020). This final product (m/z 183) has been evaluated by Zhou et al (2020) according to the Globally Harmonized System of classification and labelling of chemicals (GHS) method, showing a significantly reduced toxicity relative to the parent tetracycline (Zhou et al., 2020).

In addition to pathway PI, an additional scheme (PII) could be identified for tetracycline degradation by *M. aeruginosa* (Fig. 3a), namely, occurrence of ring-opening across the C1 and C4 positions, and fission of the double bond between C2 and C3 to form the by-product 6 (m/z 163). A further loss of N-methyl resulted in the formation of by-product 7 (m/z 149). Both tetracycline by-products 6 and 7 have been previously reported from a degradation experiment via TiO_2 photo-catalysis (Niu et al., 2013). Therefore, both degradation pathways (PI and PII) may include some processes

of photo-catalysis degradation. ~~This could be caused by the microalgae-induced indirect photo-degradation of antibiotics.~~ It has been proved that, under irradiation, the extracellular organic matters (EOMs) released by microalgae could promote the formation of active species, which may lead to indirect photo-degradation of antibiotics (Tian et al., 2019). Moreover, the ferric ion (in BG11 medium) may further react with the EOMs to generate Fe(III)-carboxylate complexes, resulting in further augmentation of the antibiotic photolysis (Wei et al., 2020). The potential photo-catalysis degradation by-products 6 and 7 ~~(m/z 163, 149) from pathway PII generated by *M. aeruginosa* were~~have been demonstrated to exhibit a decreased toxicity compared to the parent compound (Niu et al., 2013). However, a different degradation pathway (named PIII, Fig. 3b) was identified in *C. pyrenoidosa* systems, where the double bond at the C11a-C12 position was attacked by OH· to form by-product 8 (m/z 461). This molecule was then further degraded to by-product 9 (m/z 459) via hydrogen abstraction at the C5-C5a position (Ao et al., 2019). The by-products of PIII pathway (m/z 461, 459) were reported from an activated peroxymonosulfate oxidation process (Ao et al., 2019). Moreover, the by-products 8 and 9 from pathway PIII generated by *C. pyrenoidosa*, even reduced its toxicity to algae (based on the GHS evaluation), but still demonstrated the same level of toxicity to fish and daphnid according to previous studies (Pala-Ozkok et al., 2019). Therefore, the defined degradation pathway from *M. aeruginosa* treatment groups may be used to support the rapid rate of tetracycline removal and greater efficiency compared with those from the *C. pyrenoidosa* groups. Further systematic toxicity evolution experiments could help to ensure reductions in toxicity of the by-products.

3.4 Microalgae biomass and vitality response

Microalgal-based wastewater treatment offers the advantage of, in addition to the elimination of the pollutant, potential biomass re-utilization, *e.g.*, as biofuel, biochar, or fertilizer (Kim et al., 2012; Miao et al., 2004). Therefore, during the experiment, we further investigated changes occurring to the biomass, due to tetracycline exposure. Between the two algal species, *M. aeruginosa* demonstrated a better tolerance and growth recovery against tetracycline than did the *C. pyrenoidosa*. Specifically, tetracycline generated an acute inhibition on the growth of *M. aeruginosa*, at all concentrations, after one day incubation (Fig. 4a). However, the inhibition was temporary, and growth fully recovered afterwards. No significant differences in cell numbers were observed with the 10 and 50 mg L^{-1} tetracycline solutions (4.36 x 10^7 cells mL^{-1} and 3.11 x 10^7 cells mL^{-1}, respectively) which were also similar to the algal cell numbers noted in microalgal control groups (4.19 x 10^7 cells mL^{-1}, $p>0.05$) at day 11 (Fig. 4a). However, 100 mg L^{-1} tetracycline slightly inhibited biomass growth of *M. aeruginosa* ($p<0.05$) until day 11. Comparatively, all three concentrations of tetracycline inhibited the growth of *C. pyrenoidosa* to a greater extent than the microalgal control (1.74 x 10^7 cells mL^{-1}), resulting in a final value of 1.87-9.58 x 10^6 cells mL^{-1} (Fig. 4b). The results agreed well with a previous study, which revealed the inhibition, adaption, and hormesis effects of tetracycline on *M. aeruginosa* at concentrations under 10 mg L^{-1} (Ye et al., 2017). However, our study further extended the tetracycline concentration to 100 mg L^{-1}, and proved a recovery ability of *M. aeruginosa* at tetracycline concentrations under 50 mg L^{-1}.

Additionally, the results of pigment concentration (chlorophyll-a and carotenoid) and fluorescence signal intensity (Fv/Fm) analyses also agreed well with the impacts of cell number, where all tetracycline concentrations generated an acute inhibition on pigment accumulation and photosynthesis intensity (Fv/Fm). However, at tetracycline

517 concentrations under 50 mg L^{-1}, both algal species demonstrated stepwise recoveries in
518 varying degrees (Fig. S5 and S6). We concluded from these results, that *M. aeruginosa*
519 possessed a strong tetracycline removal capacity along with a higher tolerance to
520 tetracycline than did *C. pyrenoidosa*. Meanwhile, the successful recovery ability of *M.*
521 *aeruginosa* showed the potential for high biomass production, which could benefit re-
522 utilization upon completion of the treatment process.

523 *3.5 Effect of tetracycline on microcystin release*

524 As a species of cyanobacteria, *M. aeruginosa* poses a potential threat for
525 microcystin release, which may cause damage, in humans, to the liver and to the
526 nervous system (Hitzfeld et al., 2000). Consequently, we paid close attention to the
527 investigation of changes in both intercellular and released microcystin during the
528 treatment process. The study of toxin-release of *M. aeruginosa* is significant for
529 broadening the valorization of HABs species. The synthesis of microcystin is induced
530 by a mechanism protective against both abiotic and biotic stress (Babica et al., 2006)
531 and is often coupled with photosynthesis (Walls et al., 2018). Microcystin, however,
532 typically remains intracellularly, unless being released into the surroundings through
533 cell death and lysis, or as extracellular release (Paerl and Otten, 2013). In the present
534 study, at initial tetracycline concentrations of 10 and 50 mg L^{-1}, *M. aeruginosa* cells
535 analysed were in a growing or stable phase, reflected by cell growth curves (Fig. 4a).
536 Thus, intracellular microcystin-LR concentrations were generally higher than those
537 measured in the water (Fig. 5). For intracellular microcystin-LR, tetracycline inhibited
538 photosynthesis (Fig. S5a). It also exerted abiotic stress, which may have resulted in no
539 significant differences in intracellular microcystin-LR production being noted within 60
540 hours ($p>0.05$, except the systems with 100mg L^{-1} tetracycline), however, being
541 distinctly lowered over 240 hours (Fig. 5a, $p<0.05$). This reduction of induced

542 microcystin-LR may be caused by the long-term damage caused by tetracycline on the
543 synthesis of peptide synthetases, which control microcystin-LR production (Ye et al.,
544 2017).

545 The microalgal control group simulated the development of *M. aeruginosa*
546 unexposed to tetracycline, where an accelerating growth and metabolism was observed
547 (Fig. 4a). The increasing death and lysis of the cells coupled with *M. aeruginosa* growth
548 could result in an elevated microcystin-LR release into the water (Fig. 5b). Notably, an
549 overall decreasing release of microcystin-LR into the water was detected due to
550 tetracycline exposure (in the tetracycline treated groups) compared to the microalgal
551 control (except at 10 hours with 10mg L^{-1} tetracycline). This may be mainly due to the
552 reduced growth and metabolic activity of the microalgae, caused by tetracycline. The
553 rapid tetracycline removal ability of *M. aeruginosa*, which produced a removal rate of
554 over 98% in 24 hours (under 50 mg L^{-1} tetracycline) or in 48 hours (up to 100 mg L^{-1}
555 tetracycline), indicated that an optimum, but safe, treatment time for the removal of
556 tetracycline could be set at 48 hours. Within this time, the effluent with initial
557 tetracycline concentrations < 50 mg L^{-1} generated a microcystin-LR concentration lower
558 than 1 μg L^{-1} (Fig.5b). Even for wastewater containing more concentrated tetracycline
559 (up to 100 mg L^{-1}), a low-level microcystin-LR concentration of 1.8 μg L^{-1} was
560 detected in the final effluent, which was much lower than both the concentration in the
561 natural water (Christoffersen and Kaas, 2000) and the guideline concentration for
562 recreation or bathing water of Germany and Australia (< 10 μg L^{-1}) (Burch, 2008).

563 Summarily, for tetracycline concentrations in the range of 10-100 mg L^{-1}, both
564 intracellular and released microcystin-LR have been found to be reduced by varying
565 degrees. A previous study also confirmed the decrease of synthesized and released
566 microcystin-LR after tetracycline exposure (Ye et al., 2017). Regarding the effective

tetracycline removal ability even with low biomass (Fig. 1 and 4a), an appropriate decrease of the initial amount of inoculum, and timely harvest of *M. aeruginosa* cells may further ensure the effluent will conform to safe microcystin-LR levels according to the natural water and recreation or bathing water regulations. In addition, the present study also demonstrated the possibility of the long-term cultivation of low microcystin-LR *M. aeruginosa* biomass by treatment with tetracycline. Nevertheless, real-time monitoring facilities are needed for surveillance during the treatment and cultivation process in order to ensure further water security. Moreover, due to the complexity of real wastewater, where more complex compounds and other limiting factors may challenge the performance of tetracycline removal as well as release of toxin, further study is needed to investigate the efficacy and safety of the proposed approach with realistic wastewater in scaled-up systems before implementation.

3.6 Insight into future implementation

Along with the rapid development of the microalgal technology, many full-scale systems have been successfully applied for the treatment of various wastewaters, where hydraulic retention times (HRTs) were normally several days (Rawat et al., 2011; Wang et al., 2016). The current study demonstrated that *M. aeruginosa* could reduce high concentrations of tetracycline (up to 100 mg L^{-1}) down to an acceptable level (>98%) in 48 hours, which supported the feasibility of incorporatinge the process into microalgal treatment systems. Normally, such wastewaters contain both macro nutrients, *e.g.*, N and P (Wang et al., 2016), and trace elements, *e.g.*, metals (Rawat et al., 2011), which could support the growth of microalgae and result in acceptable effluent to meet discharge regulations (Wang et al., 2016). In some circumstances of wastewater with limited available nutrients, such as hospital wastewater, the nutrients could be compensated through the admixture of other high-nutritional wastewaters (Norvill et al.,

2017). Moreover, microalgae-based wastewater treatment could also provide additional benefits, such as biodiesel generation (Li et al., 2020), nutrient recovery (Chu et al., 2020), and greenhouse gas emission control (Rawat et al., 2011). The present investigation expanded the potential use of cyanobacteria for antibiotic removal at high concentrations. ~~The present investigation has preliminarily demonstrated the potential feasibility of using cyanobacteria for antibiotic removal at high concentrations.~~ HABs occur more frequently globally due to the problems of intensive eutrophication, which is detrimental to natural waters (Lyu et al., 2020). Meanwhile, wastewater contaminated with high concentrations of tetracycline, *e.g.*, pharmaceutical wastewater, livestock industry wastes, and emergency releases from hospitals, brings potential resistance-risk to the ecology. It could further impair the action of the sludge bacteria of WWTPs (Halling-Sørensen, 2001), resulting in low amounts of the tetracycline removed after treatment (Watkinson et al., 2009). By using a typical harmful algal species, *M. aeruginosa*, for the treatment of wastewater contaminated with higher concentrations of tetracycline, the problems of eutrophication and of tetracycline resistance (Fig. 6) could be simultaneously addressed.

~~Accompany with the results of current study, *M. aeruginosa* could be promising for tetracycline treatment in wastewater. However, there are still gaps between the current study and the real implementation. the high tetracycline tolerance and efficient removal rate of *M. aeruginosa* further confirmed the feasibility of this concept, which achieved a much higher tetracycline removal rat e than other investigated microalgal species (de Godos et al., 2012). In addition, tetracycline was observed to have inhibited the synthesis of microcystin-LR~~

In this study, tetracycline was observed to have inhibited the synthesis of microcystin-LR, and the effluent from the process could achieve a safe natural and

recreational water quality in respect of microcystin-LR. Notably, other trace organic and inorganic matter released by microalgae may also lead to potential risks, such as the formation of haloacetonitriles during further chlorine disinfection treatment (Pals et al., 2011). However, this has long been a common challenge for the End-of-Pipe technology of chlorine disinfection during the treatment of final wastewater effluents or of drinking water (Pals et al., 2011), which was yet covered by this study. Therefore, before the application of this treatment process, further investigations, *e.g.*, the treatment performance in real wastewater and comprehensive risk assessment are needed. ~~in realistic wastewater, and timely harvesting of the microalgal biomass for reducing the risk of such toxic release (*e.g.*, organic nitrogen, microcystin) are significant for further investigations. and with a properly managed harvest of *M. aeruginosa*, the effluent from the process could achieve a safe natural and recreational water quality in respect of microcystin-LR.~~

4. Conclusion

The present study demonstrated the possibility of reusing harmful algal species for effectively remediating high-concentration antibiotics. The harmful cyanobacterial species, *M. aeruginosa*, provided superior, efficient and rapid capacity for tetracycline removal, compared with *C. pyrenoidosa*, under a wide initial concentration range (10-100 mg L^{-1}). Both microalgal species promoted tetracycline hydrolysis by raising the water pH, however, biodegradation contributed to the major part of the removal by *M. aeruginosa*. Both microalgae species shared a common tetracycline degradation pathway, but also utilised unique species-specific pathways producing different degradation by-products. The by-products showed no significant increase of toxicity according to published references. The presence of the tetracycline could have

significantly inhibited the release of toxic microcystin-LR into the water, thus promoting the relative safety of the final effluent after treatment. Notably, the current study was carried out in the synthetic antibiotic-contaminated water, which provided evidence-based insights into the proposed approach. However, further study is needed in order to evaluate the performance with realistic wastewater in upscaled systems prior to practical implementation.

Declaration of competing interest

The authors declare that they have no known competing financial interests or personal relationships that could have appeared to influence the work reported in this paper

Acknowledgements

The research was supported by the National Key R&D Program of China (2017YFA0207204). The PhD fellowship of Minmin Pan was supported by the China Scholarship Council (CSC). We also thank the Danish Innovation Foundation for support through the InWAP project.

Reference

Ao, X., Sun, W., Li, S., Yang, C., Li, C., Lu, Z., 2019. Degradation of tetracycline by medium pressure UV-activated peroxymonosulfate process: Influencing factors, degradation pathways, and toxicity evaluation. Chem. Eng. J. 361, 1053–1062.

Arbib, Z., Ruiz, J., Álvarez-Díaz, P., Garrido-Pérez, C., Perales, J.A., 2014. Capability of different microalgae species for phytoremediation processes: Wastewater tertiary treatment, CO2 bio-fixation and low cost biofuels production. Water Res. 49, 465–474.

Babica, P., Bláha, L., Maršálek, B., 2006. Exploring the natural role of microcystins—A review of effects on photoautotrophic organisms 1. J. Phycol. 42, 9–20.

Burch, M.D., 2008. Effective doses, guidelines & regulations, in: Cyanobacterial Harmful Algal Blooms: State of the Science and Research Needs. Springer, pp. 831–853.

667 Cao, M., Wang, P., Ao, Y., Wang, C., Hou, J., Qian, J., 2016. Visible light activated
668 photocatalytic degradation of tetracycline by a magnetically separable composite
669 photocatalyst: graphene oxide/magnetite/cerium-doped titania. J. Colloid Interface Sci.
670 467, 129–139.
671 Choi, Y.-K., Choi, T.-R., Gurav, R., Bhatia, S.K., Park, Y.-L., Kim, H.J., Kan, E., Yang, Y.-H.,
672 2020. Adsorption behavior of tetracycline onto Spirulina sp.(microalgae)-derived biochars
673 produced at different temperatures. Sci. Total Environ. 710, 136282.
674 Christoffersen, K., Kaas, H., 2000. Toxic cyanobacteria in water. A guide to their public health
675 consequences, monitoring, and management. Limnol. Oceanogr. 45, 1212.
676 Chu, Q., Lyu, T., Xue, L., Yang, L., Feng, Y., Sha, Z., Yue, B., Mortimer, R.J.G., Cooper, M.,
677 Pan, G., 2020. Hydrothermal carbonization of microalgae for phosphorus recycling from
678 wastewater to crop-soil systems as slow-release fertilizers. J. Clean. Prod. 124627.
679 Daghrir, R., Drogui, P., 2013. Tetracycline antibiotics in the environment: a review. Environ.
680 Chem. Lett. 11, 209–227.
681 de Godos, I., Muñoz, R., Guieysse, B., 2012. Tetracycline removal during wastewater treatment
682 in high-rate algal ponds. J. Hazard. Mater. 229, 446–449.
683 Fu, Y., Peng, L., Zeng, Q., Yang, Y., Song, H., Shao, J., Liu, S., Gu, J., 2015. High efficient
684 removal of tetracycline from solution by degradation and flocculation with nanoscale
685 zerovalent iron. Chem. Eng. J. 270, 631–640.
686 Gao, Y., Li, Y., Zhang, L., Huang, H., Hu, J., Shah, S.M., Su, X., 2012. Adsorption and removal
687 of tetracycline antibiotics from aqueous solution by graphene oxide. J. Colloid Interface
688 Sci. 368, 540–546.
689 Guo, H., Niu, C.-G., Zhang, L., Wen, X.-J., Liang, C., Zhang, X.-G., Guan, D.-L., Tang, N.,
690 Zeng, G.-M., 2018. Construction of direct Z-scheme AgI/Bi2Sn2O7 nanojunction system
691 with enhanced photocatalytic activity: accelerated interfacial charge transfer induced
692 efficient Cr (VI) reduction, tetracycline degradation and Escherichia coli inactivation.
693 ACS Sustain. Chem. Eng. 6, 8003–8018.

694 Halling-Sørensen, B., 2001. Inhibition of aerobic growth and nitrification of bacteria in sewage
695 sludge by antibacterial agents. Arch. Environ. Contam. Toxicol. 40, 451–460.
696 Halling-Sørensen, B., Sengeløv, G., Tjørnelund, J., 2002. Toxicity of tetracyclines and
697 tetracycline degradation products to environmentally relevant bacteria, including selected
698 tetracycline-resistant bacteria. Arch. Environ. Contam. Toxicol. 42, 263–271.
699 Hitzfeld, B.C., Höger, S.J., Dietrich, D.R., 2000. Cyanobacterial toxins: removal during
700 drinking water treatment, and human risk assessment. Environ. Health Perspect. 108, 113–
701 122.
702 Hongyang, S., Yalei, Z., Chunmin, Z., Xuefei, Z., Jinpeng, L., 2011. Cultivation of Chlorella
703 pyrenoidosa in soybean processing wastewater. Bioresour. Technol. 102, 9884–9890.
704 Hou, L., Wang, L., Royer, S., Zhang, H., 2016. Ultrasound-assisted heterogeneous Fenton-like
705 degradation of tetracycline over a magnetite catalyst. J. Hazard. Mater. 302, 458–467.
706 Huang, D., Li, J., Zeng, G., Xue, W., Chen, S., Li, Z., Deng, R., Yang, Y., Cheng, M., 2019.
707 Facile construction of hierarchical flower-like Z-scheme AgBr/Bi2WO6 photocatalysts for
708 effective removal of tetracycline: Degradation pathways and mechanism. Chem. Eng. J.
709 375, 121991.
710 Jiao, S., Zheng, S., Yin, D., Wang, L., Chen, L., 2008. Aqueous photolysis of tetracycline and
711 toxicity of photolytic products to luminescent bacteria. Chemosphere 73, 377–382.
712 Kim, J.D., Yoon, Y.H., Shin, T.S., Kim, M.Y., Seo, H.J., 2012. Bioalcohol production with M.
713 aeruginosa as a novel resource, in: 2012 Oceans-Yeosu. IEEE, pp. 1–10.
714 Kim, S., Eichhorn, P., Jensen, J.N., Weber, A.S., Aga, D.S., 2005. Removal of antibiotics in
715 wastewater: effect of hydraulic and solid retention times on the fate of tetracycline in the
716 activated sludge process. Environ. Sci. Technol. 39, 5816–5823.
717 Li, G., Zhang, J., Li, H., Hu, R., Yao, X., Liu, Y., Zhou, Y., Lyu, T., 2020. Towards high-
718 quality biodiesel production from microalgae using original and anaerobically-digested
719 livestock wastewater. Chemosphere 128578.
720 Lyu, T., Song, L., Chen, Q., Pan, G., 2020. Lake and River Restoration: Method, Evaluation and

721 Management.
722 Matamoros, V., Uggetti, E., García, J., Bayona, J.M., 2016. Assessment of the mechanisms
723 involved in the removal of emerging contaminants by microalgae from wastewater: a
724 laboratory scale study. J. Hazard. Mater. 301, 197–205.
725 Miao, X., Wu, Q., Yang, C., 2004. Fast pyrolysis of microalgae to produce renewable fuels. J.
726 Anal. Appl. Pyrolysis 71, 855–863.
727 Niu, J., Ding, S., Zhang, L., Zhao, J., Feng, C., 2013. Visible-light-mediated Sr-Bi2O3
728 photocatalysis of tetracycline: kinetics, mechanisms and toxicity assessment.
729 Chemosphere 93, 1–8.
730 Norvill, Z.N., Toledo-Cervantes, A., Blanco, S., Shilton, A., Guieysse, B., Muñoz, R., 2017.
731 Photodegradation and sorption govern tetracycline removal during wastewater treatment in
732 algal ponds. Bioresour. Technol. 232, 35–43.
733 Paerl, H.W., Otten, T.G., 2013. Harmful cyanobacterial blooms: causes, consequences, and
734 controls. Microb. Ecol. 65, 995–1010.
735 Pala-Ozkok, I., Ubay-Cokgor, E., Jonas, D., Orhon, D., 2019. Kinetic and microbial response of
736 activated sludge community to acute and chronic exposure to tetracycline. J. Hazard.
737 Mater. 367, 418–426.
738 Pals, J.A., Ang, J.K., Wagner, E.D., Plewa, M.J., 2011. Biological mechanism for the toxicity of
739 haloacetic acid drinking water disinfection byproducts. Environ. Sci. Technol. 45, 5791–
740 5797.
741 Pan, G., Lyu, T., Mortimer, R., 2018. Comment: Closing phosphorus cycle from natural waters:
742 Re-capturing phosphorus through an integrated water-energy-food strategy. J. Environ. Sci.
743 65, 375–376.
744 Qian, H., Li, J., Pan, X., Sun, Z., Ye, C., Jin, G., Fu, Z., 2012. Effects of streptomycin on
745 growth of algae Chlorella vulgaris and Microcystis aeruginosa. Environ. Toxicol. 27, 229–
746 237.
747 Rawat, I., Kumar, R.R., Mutanda, T., Bux, F., 2011. Dual role of microalgae: phycoremediation

748 of domestic wastewater and biomass production for sustainable biofuels production. Appl.
749 Energy 88, 3411–3424.
750 Rzymski, P., Niedzielski, P., Karczewski, J., Poniedziałek, B., 2014. Biosorption of toxic metals
751 using freely suspended Microcystis aeruginosa biomass. Open Chem. 12, 1232–1238.
752 Sarmah, A.K., Meyer, M.T., Boxall, A.B.A., 2006. A global perspective on the use, sales,
753 exposure pathways, occurrence, fate and effects of veterinary antibiotics (VAs) in the
754 environment. Chemosphere 65, 725–759.
755 Shen, Hongqiang, Liu, G., Zhao, Y., Li, D., Jiang, J., Ding, J., Mao, B., Shen, Hao, Kim, K.-S.,
756 Shi, W., 2020. Artificial all-solid-state system by RGO bridged Cu2O and Bi2WO6 for Z-
757 scheme H2 production and tetracycline degradation. Fuel 259, 116311.
758 Song, Z., Ma, Y. L., Li, C. E., 2019. The residual tetracycline in pharmaceutical wastewater was
759 effectively removed by using MnO2/graphene nanocomposite. Sci. Total Environ. 651,
760 580–590.
761 Suárez, S., Carballa, M., Omil, F., Lema, J.M., 2008. How are pharmaceutical and personal care
762 products (PPCPs) removed from urban wastewaters? Rev. Environ. Sci. Bio/Technology 7,
763 125–138.
764 Tang, L., Wang, Jiajia, Zeng, G., Liu, Y., Deng, Y., Zhou, Y., Tang, J., Wang, Jingjing, Guo, Z.,
765 2016. Enhanced photocatalytic degradation of norfloxacin in aqueous Bi2WO6 dispersions
766 containing nonionic surfactant under visible light irradiation. J. Hazard. Mater. 306, 295–
767 304.
768 Tian, Y., Zou, J., Feng, L., Zhang, L., Liu, Y., 2019. Chlorella vulgaris enhance the
769 photodegradation of chlortetracycline in aqueous solution via extracellular organic matters
770 (EOMs): Role of triplet state EOMs. Water Res. 149, 35–41.
771 Walls, J.T., Wyatt, K.H., Doll, J.C., Rubenstein, E.M., Rober, A.R., 2018. Hot and toxic:
772 Temperature regulates microcystin release from cyanobacteria. Sci. Total Environ. 610,
773 786–795.
774 Wan, J., Guo, P., Peng, X., Wen, K., 2015. Effect of erythromycin exposure on the growth,

775 antioxidant system and photosynthesis of Microcystis flos-aquae. J. Hazard. Mater. 283,
776 778–786.
777 Wang, M., Yang, Y., Chen, Z., Chen, Y., Wen, Y., Chen, B., 2016. Removal of nutrients from
778 undiluted anaerobically treated piggery wastewater by improved microalgae. Bioresour.
779 Technol. 222, 130–138.
780 Wang, X., Wang, Y., Li, D., 2013. Degradation of tetracycline in water by ultrasonic irradiation.
781 Water Sci. Technol. 67, 715–721.
782 Watkinson, A.J., Murby, E.J., Kolpin, D.W., Costanzo, S.D., 2009. The occurrence of
783 antibiotics in an urban watershed: from wastewater to drinking water. Sci. Total Environ.
784 407, 2711–2723.
785 Wei, L., Li, H., Lu, J., 2020. Algae-induced photodegradation of antibiotics: a review. Environ.
786 Pollut. 115589.
787 Xiong, J.-Q., Kurade, M.B., Jeon, B.-H., 2017a. Biodegradation of levofloxacin by an
788 acclimated freshwater microalga, Chlorella vulgaris. Chem. Eng. J. 313, 1251–1257.
789 Xiong, J.-Q., Kurade, M.B., Kim, J.R., Roh, H.-S., Jeon, B.-H., 2017b. Ciprofloxacin toxicity
790 and its co-metabolic removal by a freshwater microalga Chlamydomonas mexicana. J.
791 Hazard. Mater. 323, 212–219.
792 Yang, W., Tang, Z., Zhou, F., Zhang, W., Song, L., 2013. Toxicity studies of tetracycline on
793 Microcystis aeruginosa and Selenastrum capricornutum. Environ. Toxicol. Pharmacol. 35,
794 320–324.
795 Ye, J., Du, Y., Wang, L., Qian, J., Chen, J., Wu, Q., Hu, X., 2017. Toxin release of
796 cyanobacterium Microcystis aeruginosa after exposure to typical tetracycline antibiotic
797 contaminants. Toxins (Basel). 9, 53.
798 Yi, Q., Gao, Y., Zhang, Hong, Zhang, Haifeng, Zhang, Y., Yang, M., 2016. Establishment of a
799 pretreatment method for tetracycline production wastewater using enhanced hydrolysis.
800 Chem. Eng. J. 300, 139–145.
801 Zhang, H., Shang, Y., Lyu, T., Chen, J., Pan, G., 2018. Switching harmful algal blooms to

submerged macrophytes in shallow waters using geo-engineering methods: Evidence from a 15N tracing study. Environ. Sci. Technol. 52, 11778–11785.

Zhou, J., Ma, F., Guo, H., Su, D., 2020. Activate hydrogen peroxide for efficient tetracycline degradation via a facile assembled carbon-based composite: Synergism of powdered activated carbon and ferroferric oxide nanocatalyst. Appl. Catal. B Environ. 269, 118784.

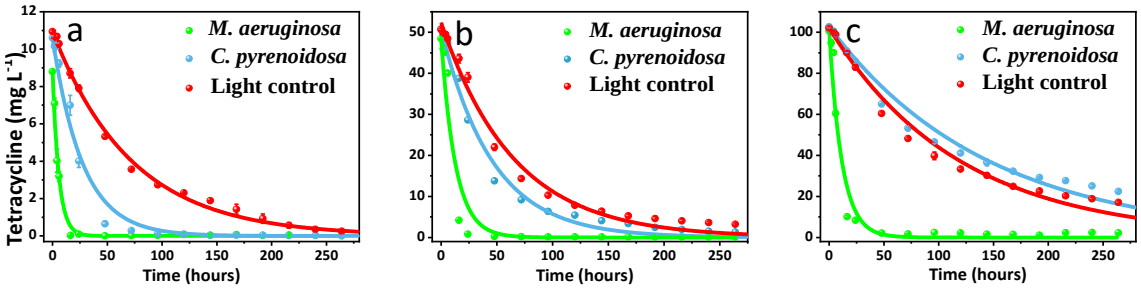

Fig. 1. The dynamics of tetracycline concentration in blank control groups, and treatment groups of *M. aeruginosa* and *C. pyrenoidosa* at initial concentrations of 10 mg L^{-1} (a), 50 mg L^{-1} (b), and 100 mg L^{-1} (c). The solid lines are simulated pseudo-first-order kinetic degradation models.

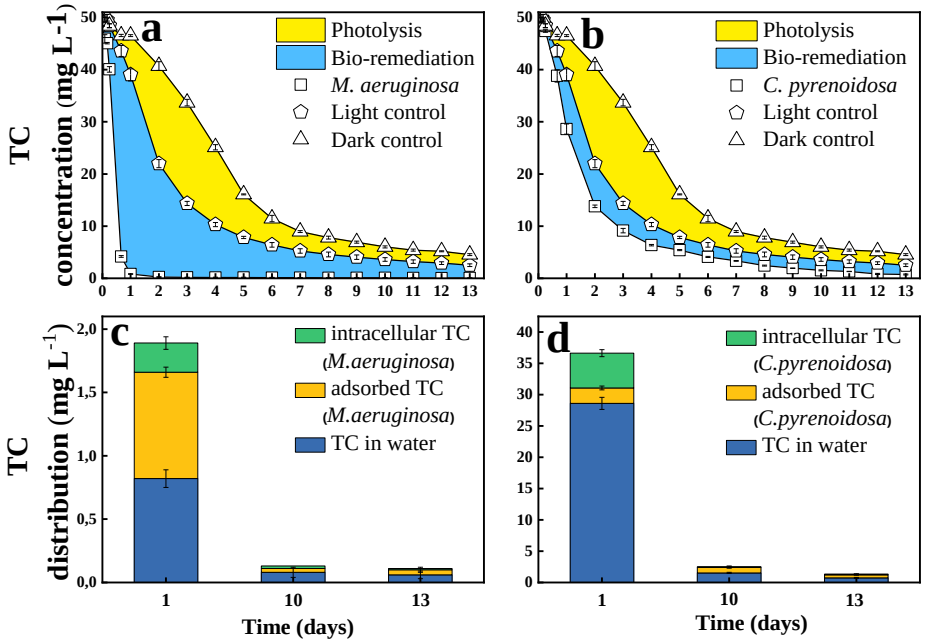

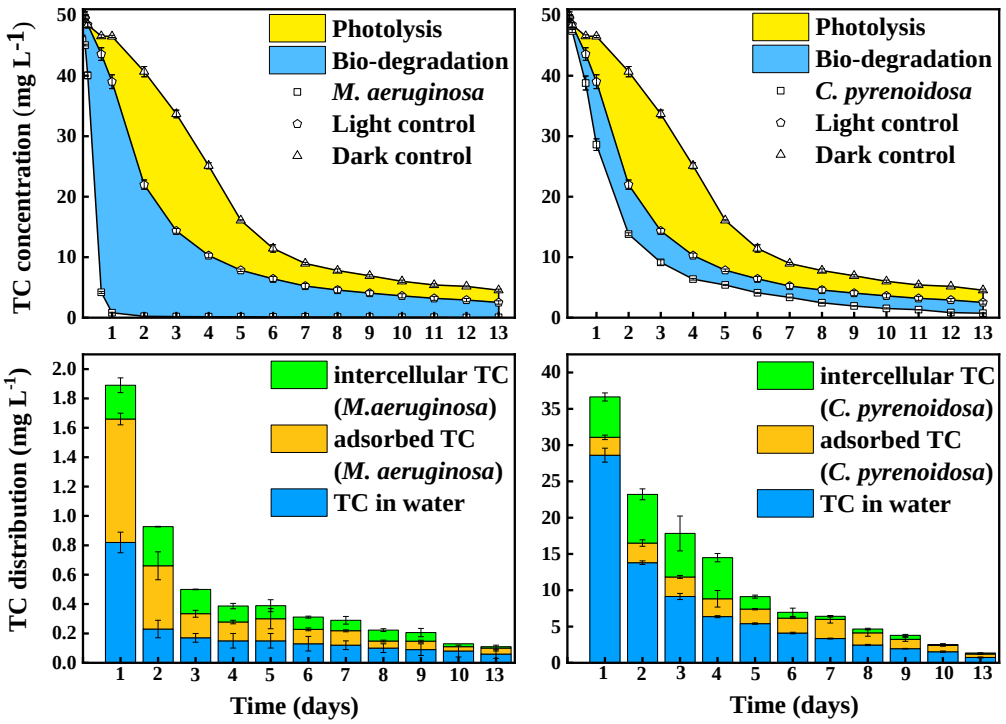

Fig. 2. Theoretically different contributions (photolysis, hydrolysis & cation-binding and bio-remediation) towards tetracycline removal in (a) *M. aeruginosa*, and (b) *C. pyrenoidosa* treatment groups, and distribution (in water, adsorption by microalgae and bio-accumulation into microalgal cells) of residual tetracycline in (c) *M. aeruginosa*, and (d) *C. pyrenoidosa* treatment groups.

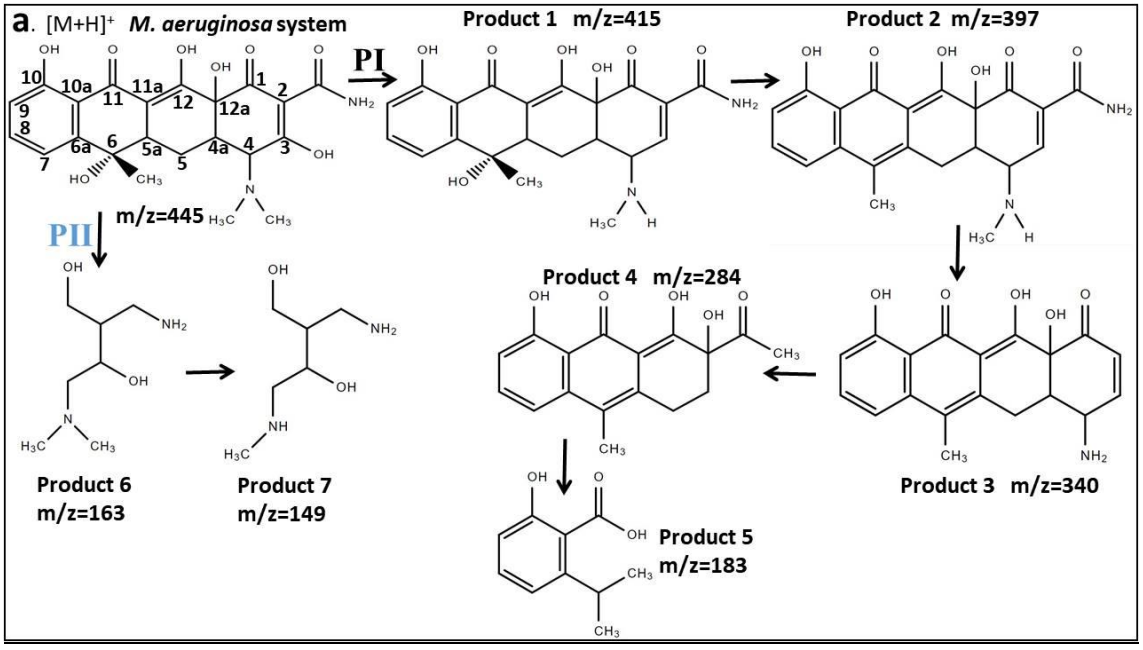

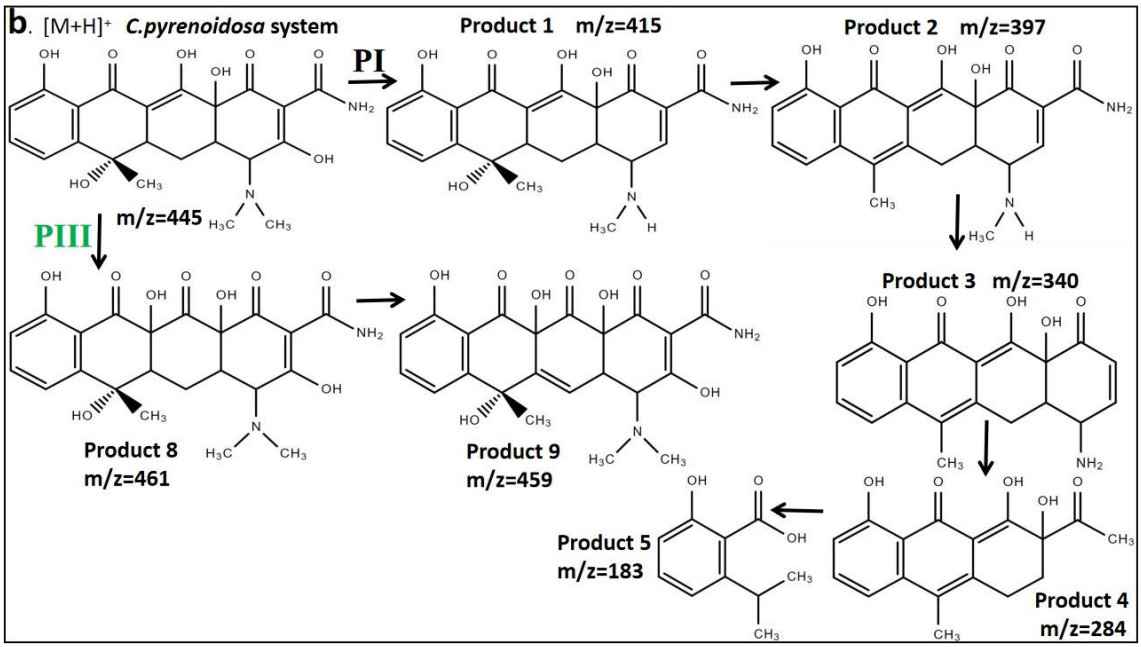

Fig. 3. Tetracycline degradation by-products and potential pathways (PI, PII, and PIII) in (a) *M. aeruginosa*, and (b) *C. pyrenoidosa* treatment groups.

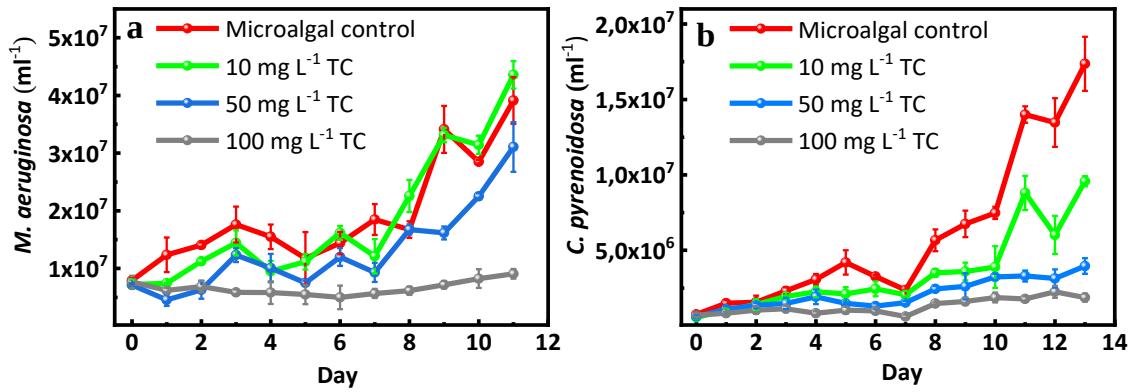

Fig. 4. Cell number growth under varying tetracycline concentrations for (a) *M. aeruginosa*, and (b) *C. pyrenoidosa* treatment groups.

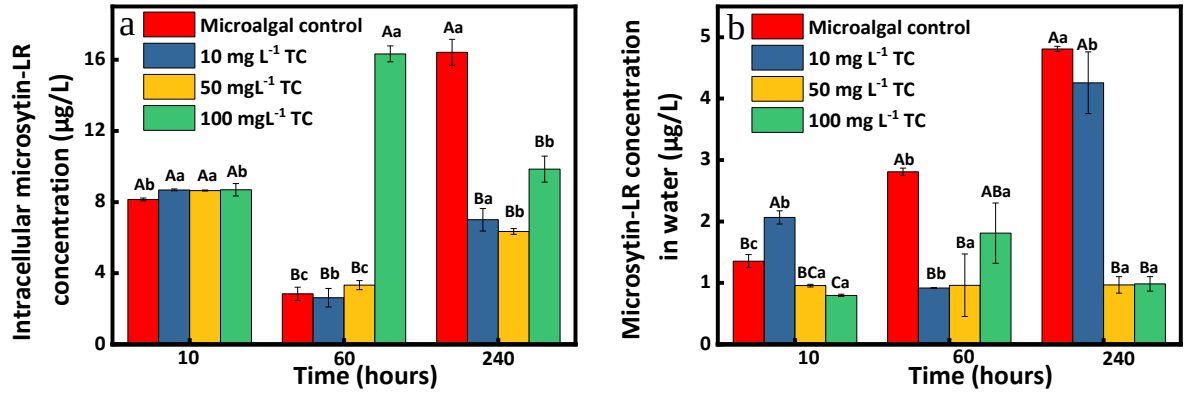

Fig. 5. Microcystin-LR concentrations of (a) intracellular *M. aeruginosa*, and (b) released into water from *M. aeruginosa*. Different uppercase letters above the error bars in each figure represent significant difference ($p < 0.05$) among different treatment groups at the same sampling time. Different lowercase letters above error bars in each figure represent significant difference ($p < 0.05$) of the same treatment group over different sampling times.

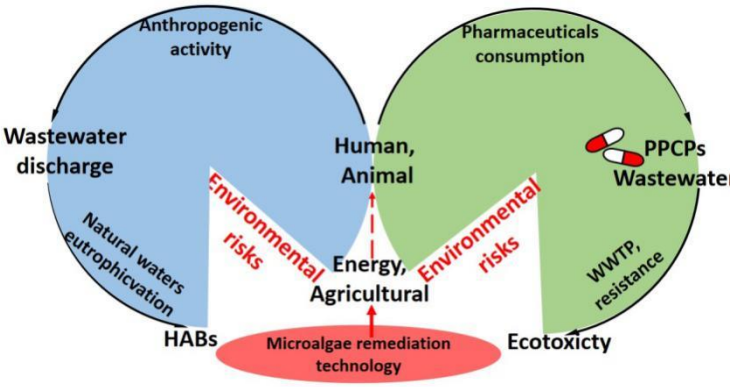

Fig. 6. Sustainable microalgae remediation strategy for addressing the environmental problems caused by pharmaceuticals and personal care products (PPCPs) and Harmful Algae Blooms (HABs).

Table 1 Pseudo-first-order kinetic model fitting results of tetracycline removal.

Tetracycline removal	Initial tetracycline concentration (mg L^{-1})	k value	R^2
M. aeruginosa	10	$(1.7 \pm 0.1) \times 10^{-1}$	0.99
	50	$(7.7 \pm 1.3) \times 10^{-2}$	0.94
	100	$(8.6 \pm 1.0) \times 10^{-2}$	0.97
C. pyrenoidosa	10	$(3.6 \pm 0.3) \times 10^{-2}$	0.99
	50	$(2.2 \pm 1.1) \times 10^{-2}$	0.99
	100	$(7.0 \pm 0.3) \times 10^{-3}$	0.98
Control	10	$(1.4 \pm 0.0) \times 10^{-2}$	0.99
	50	$(1.5 \pm 0.1) \times 10^{-2}$	0.99
	100	$(8.4 \pm 0.4) \times 10^{-3}$	0.98

Supplementary information

Mitigating antibiotic pollution using cyanobacteria: removal efficiency, pathways and metabolism

Minmin Pan[a,b,c], Tao Lyu*[,d], Lumeng Zhan[a,b], Victor Matamoros[e], Irini Angelidaki[c], Mick Cooper[f], Gang Pan*[,a,b,f]

[a]*Research Center for Eco-Environmental Sciences, Chinese Academy of Sciences, Beijing 100085, China*

[b]*Sino-Danish College of University of Chinese Academy of Sciences, Beijing 100049, China*

[c]*Department of Environmental Engineering, Technical University of Denmark, DK-2899 Lyngby, Denmark*

[d]*Cranfield Water Science Institute, Cranfield University, College Road, Cranfield, Bedfordshire MK43 0AL, UK*

[e]*Department of Environmental Chemistry, IDAEA-CSIC, Jordi Girona, 18-26, E-08034 Barcelona, Spain*

[f]*School of Animal, Rural and Environmental Sciences, Nottingham Trent University, Brackenhurst Campus, NG25 0QF, UK*

**Corresponding authors*: gang.pan@ntu.ac.uk (G. Pan); t.lyu@cranfield.ac.uk (T. Lyu).

S1. Materials and methods

S1.1 Sample preparation and tetracycline detection

Standard tetracycline hydrochloride was purchased from J&K Scientific Ltd., Beijing, China. Prior to the determination, samples were filtered using a membrane filter (0.22µm). The Acquity UPLC-PDA (Diode Array Detector) analysis parameters for UV detection of tetracycline were as follows: wavelength 355nm (4.8 nm resolution), sample temperature 10^{o}C and column temperature 35^{o}C. The following was used as the mobile phase: 0.2% formic acid in ultrapure water (A) and acetonitrile (B). The eluent flow rate was 0.4 mL min^{-1}. A gradient ratio of A 90%: B 10% to A 10%: B 90% was applied over 4 min.10µL of sample was taken for each injection. Before each determination, the analytical precision was checked with three levels of tetracycline (0.5, 5, 50 mg L^{-1}). The results showed a relative standard deviation (RSD%) to be in the range of between 4.3-8.7%.

Samples of treated wastewater (2mL) were taken at ~~days~~ hours 1/6, 1/3, 1, 2, 4, 10, 20, 24, 36, and daily from day 2 to 13, and pre-treated by centrifugation at 8000 rpm for 15min, thus isolating the microalgae cells. The supernatant was then passed through a membrane filter (0.22µm) for the detection of tetracycline concentration in water. After re-suspension of the microalgae pellet into ultrapure water (5ml) and re-centrifugation, the supernatant was measured in order to quantify the bio-adsorption of tetracycline. The microalgal pellets were finally homogenised into a mixture of methanol and dichloromethane (5ml; 2:1 v/v) followed by 40 minutes sonication (60kHz). After subsequent centrifugation, the supernatant was analysed to determine the concentration of bioaccumulated tetracycline.

S1.2 Sample preparation and detection of tetracycline by-products

A UPLC (Acquity UPLC I-Class, Waters Corp., Milford, USA) coupled with a Xevo G2 ToF-MS (Waters Corp., USA) was utilised for the analysis of tetracycline degradation products. Prior to analysis, samples were initially pre-concentrated by treatment with SPE Oasis solid-phase extraction sorbents (Oasis R MCX 6cc (500mg) LP extraction cartridges, Waters Corp., Milford, USA). For ToF-MS detection, effluent A and B were 0.1% formic acid in ultrapure water and pure acetonitrile, respectively. The flow speed was 0.4 ml min-1, a gradient of flowing phase A and B from initial ratio of 90% : 10% to 10% : 90% was set within 10 min and kept the final ratio until 30 min. Mass spectrometry conditions were as follows: detection time 30min, acquisition mass range 50 to 1200 Da, scan time 1.5 sec, collision energy 6V, collision energy ramp from 15 to 30V, cone voltage 40 V, positive polarity, analyse mode resolution, dynamic range normal.

S1.3 Sample preparation and microcystin detection

In this study, the most toxic microcystin compound, microcystin-LR (MC-LR), was analysed for both intracellular and extracellular concentrations. Specifically, 50ml of sample was centrifuged (4800rpm for 15min) and MC-LR in the supernatant was initially concentrated by SPE (Oasis R MCX 6cc, 500mg, LP extraction cartridges; Waters Corp., Milford, USA), 10ml 100% methanol was used to activate the SPE, following by a wash-out of 20ml ultrapure water with a speed of 3ml min^{-1}. Afterwards, the supernatant was flowing through the activated SPE with a speed of 1ml min^{-1}. 10ml ultrapure water, 20ml 5%, 15% and 20% (v/v) methanol were utilized for the wash-out of impurities, following by a speed of 1ml min^{-1} 35% (v/v) 3ml methanol to elute the MC-LR. The 3ml eluent was then flushed with nitrogen with a temperature of 25℃ to 1.2ml. Final sample was further filtered with 0.22μm filter before the injection into the UPLC.

For the intracellular MC-LR concentration, the pellet was first washed three times with ultrapure water and then dissolved with 80% (v/v) methanol and freeze-thawing with liquid nitrogen three times to break the microalgae cells and extract the intracellular MC-LR, finally 1ml concentrated sample was achieved by nitrogen flushing in room temperature. The samples were further filtered with 0.22μm filter before the detection by Acquity UPLC. For the Acquity UPLC detection, For microcystin-LR detection, 0.5% trifluoroacetic acid (A) and pure acetonitrile (B) were used as mobile phases, with a gradient from A60%:B40% to A40%:B60%. The working parameters were set as: flow rate 0.5 mL min^{-1}, 30 °C column temperature and 10 °C sample temperature, detector wavelength 238 nm (1.2 nm resolution).

S1.4 Sampling and pigments detection

At day 1, 3, 6 and 10, cell pigments were firstly extracted with methanol (10 mL, 90% v/v), and the concentrations of chlorophyll and carotenoids were determined by UV spectrophotometer (Varian Cary 50; Agilent Instruments, Santa Clara, USA) measuring the absorbance at wavelengths of 665, 652 and 470nm. Based on the equation (1-3) below, the concentrations were calculated:

$$C_a=16.82A_{665.2}-9.28A_{652.4} \quad \text{(S2)}$$

$$C_b=36.92A_{652.4}-16.54A_{665.2} \quad \text{(S3)}$$

$$C_{carotenoid}=\frac{1000A470-1.91Ca-1.91Cb}{225} \quad \text{(S4)}$$

where, C_a and C_b (mg L^{-1}) are the concentrations of the chlorophyll-a and chlorophyll-b, $C_{carotenoid}$ (mg L^{-1}) represents the concentration of carotenoid pigment.

S1.5 Sampling and photosynthesis intensity detection

Samples of 1 mL was taken daily from each flasks for the photosynthesis intensity detection. Photosynthesis intensity parameter Fv/Fm was measured using a FluorPen (FP100, PSI spol.s.r.o., Drasov, Czechia), of which a 10 min dark adaption phase for each sample was conducted before the measurement.

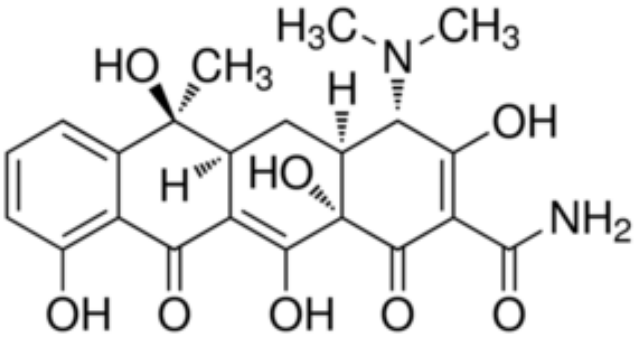

Fig. S1. Molecular structure of tetracycline

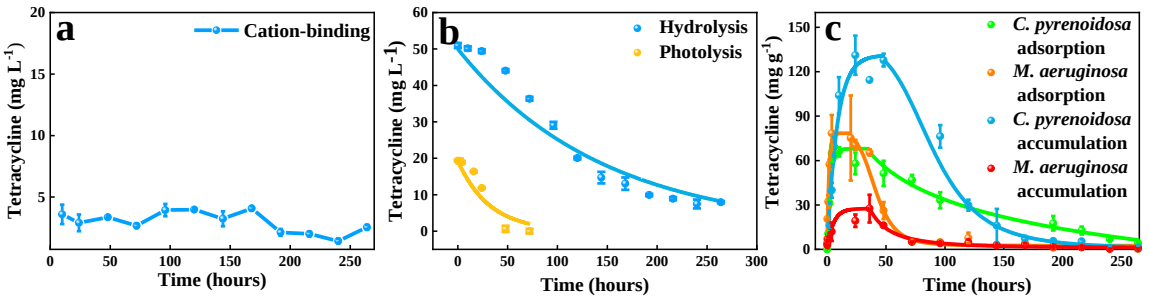

Fig.S2. Kinetic study of different contributions towards tetracycline removal of (a) ascent stage of bio-adsorption and bio-accumulation, (b) declining stage of bio-adsorption and bio-accumulation, (c) hydrolysis and photolysis and (d) cation-binding. The solid lines in (a), (b) and (c) are simulated pseudo-first-order kinetic degradation models.

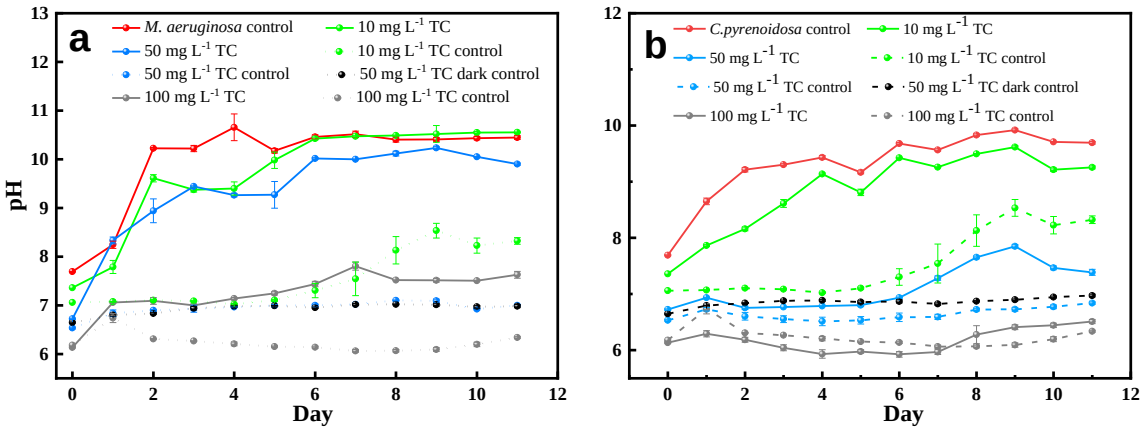

988

989 **Fig. ~~S2~~S3.** pH changes under varying tetracycline concentrations in (a) *M. aeruginosa* treatment

990 groups, and (b) *C. pyrenoidosa* treatment groups.

991

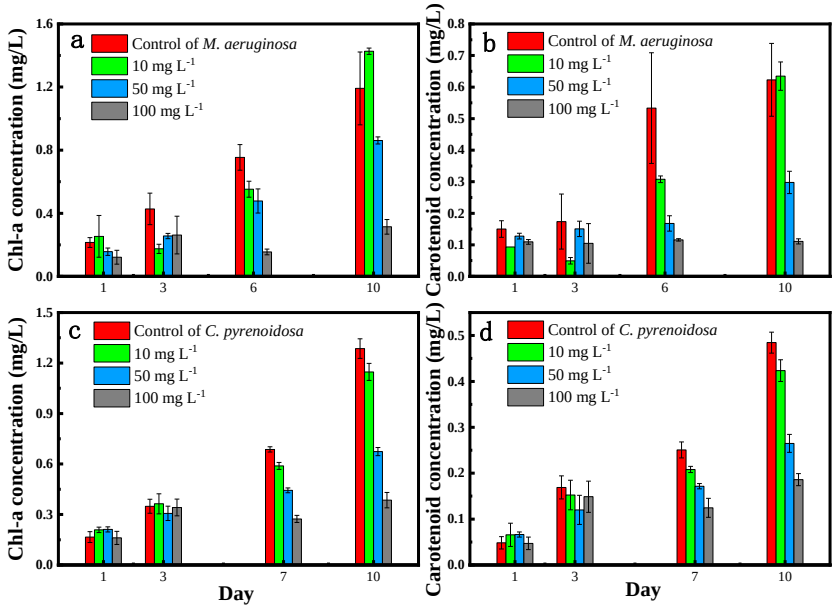

992

993 **Fig. S4**. Chlorophyll-a concentration changes in (a) *M. aeruginosa* treatment groups,

994 and (c) *C. pyrenoidosa* treatment groups, and Carotenoid concentration changes in (b)

995 *M. aeruginosa* treatment groups and (d) *C. pyrenoidosa* treatment groups.

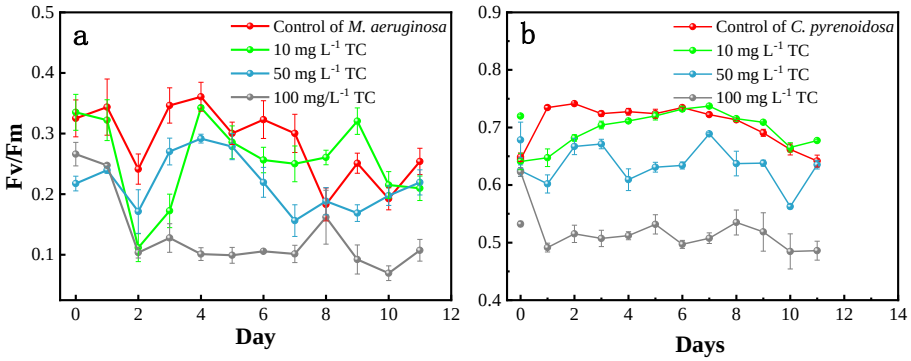

996

997 **Fig. S5.** Fluorescence intensity changes of Fv/Fm under varying tetracycline concentrations in

998 (a) *M. aeruginosa* treatment groups, and (b) *C. pyrenoidosa* treatment groups

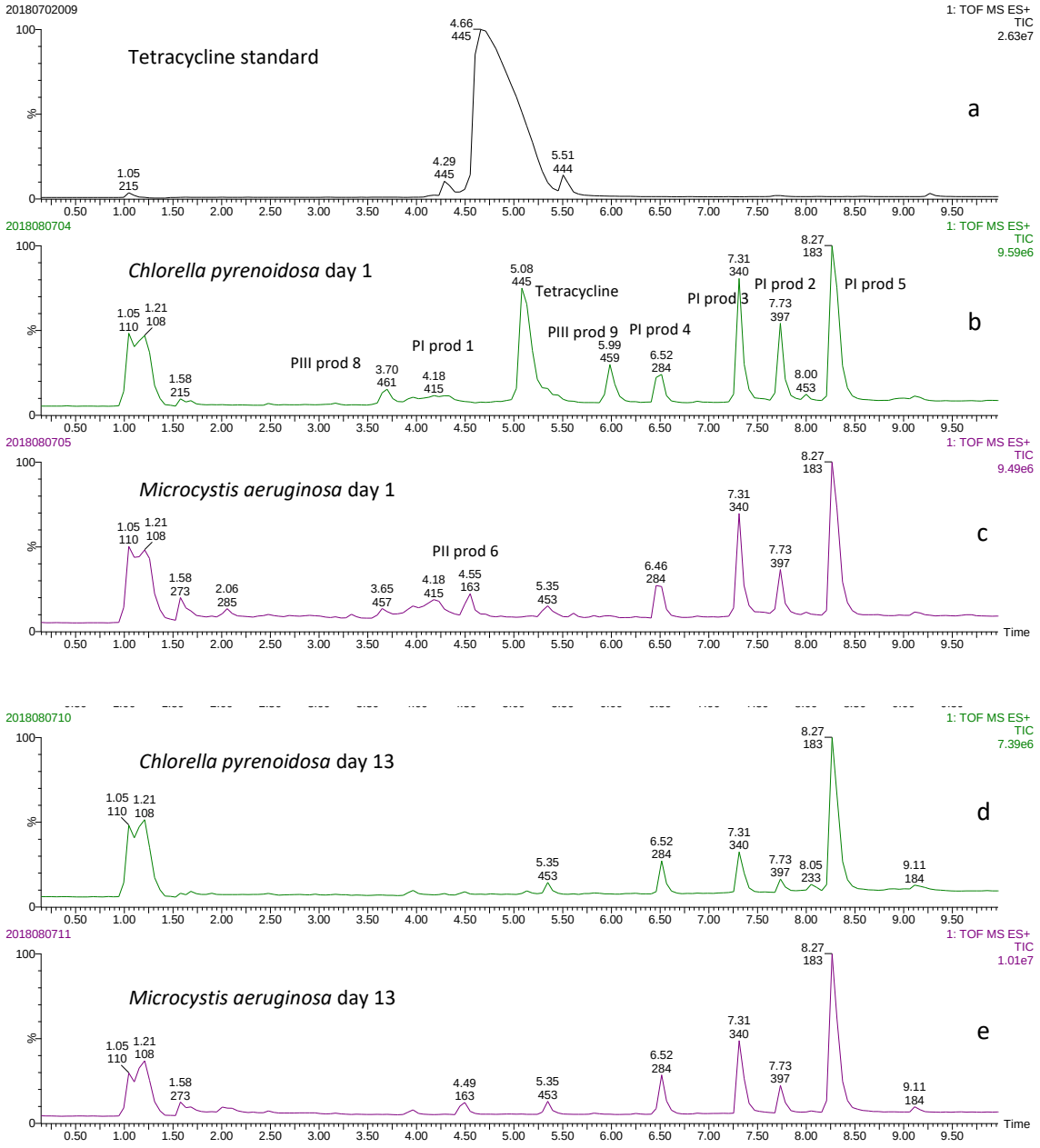

Fig. ~~S3~~S6. LC-ToFMS chromatograms of tetracycline (a) and degradation by-products from the *C. pyrenoidosa* (b; day 1 & d; day 13) and *M. aeruginosa* (c; day 1 & e; day 13) treatment groups. Chromatographic peak labels indicate retention time in minutes (top number) and base peak mass (lower number). Peaks with the same retention time and base peak mass represent the same compounds. Additional peak labels in chromatograms b and c indicate compound identifications according to degradation pathways illustrated in Fig. 3.

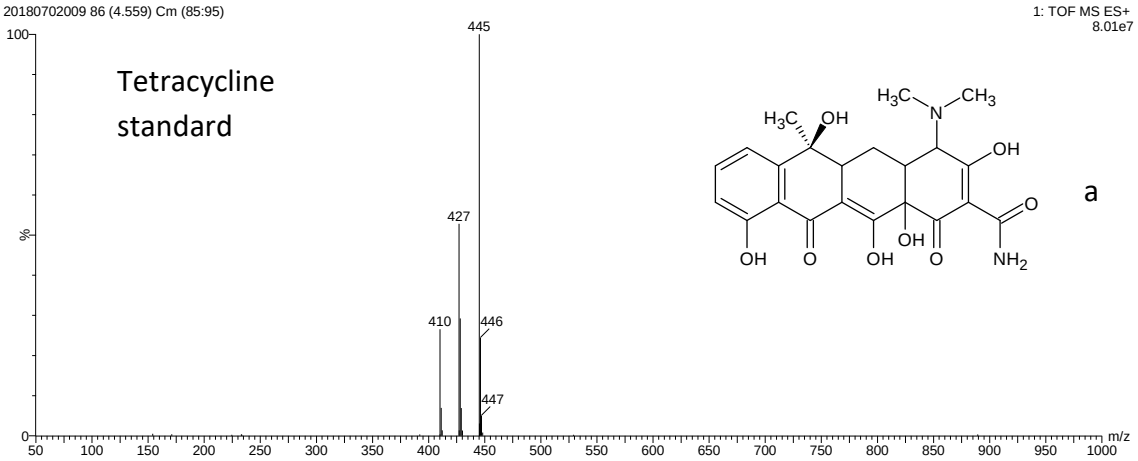

1007

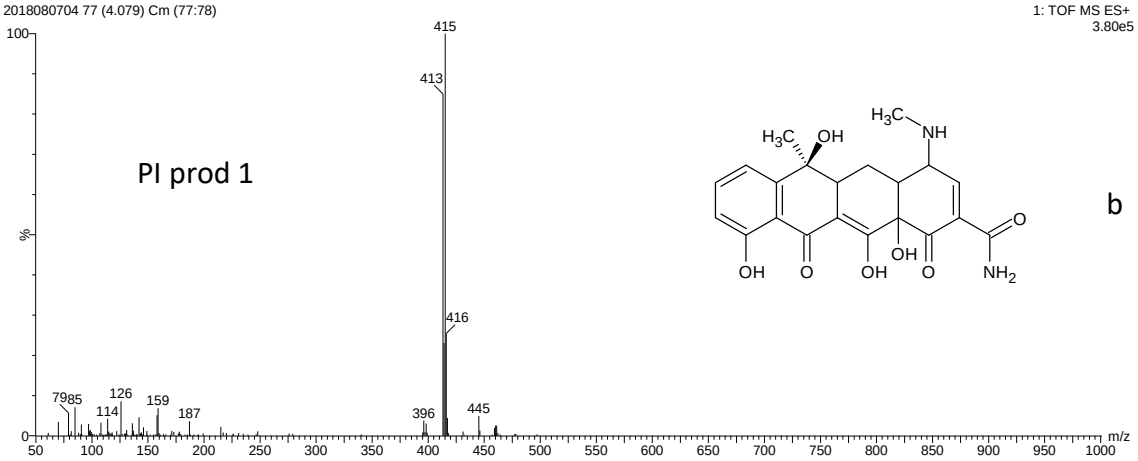

1008

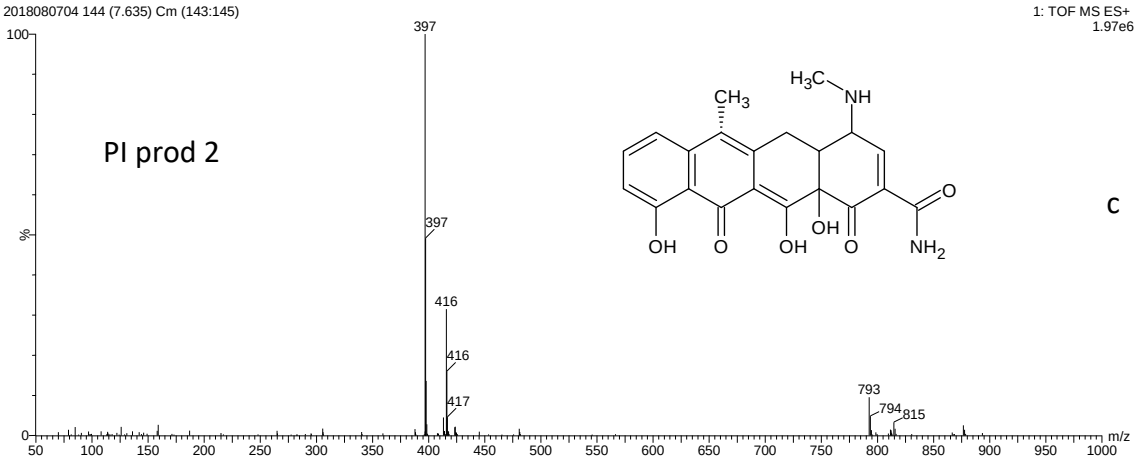

1009

1010

1011

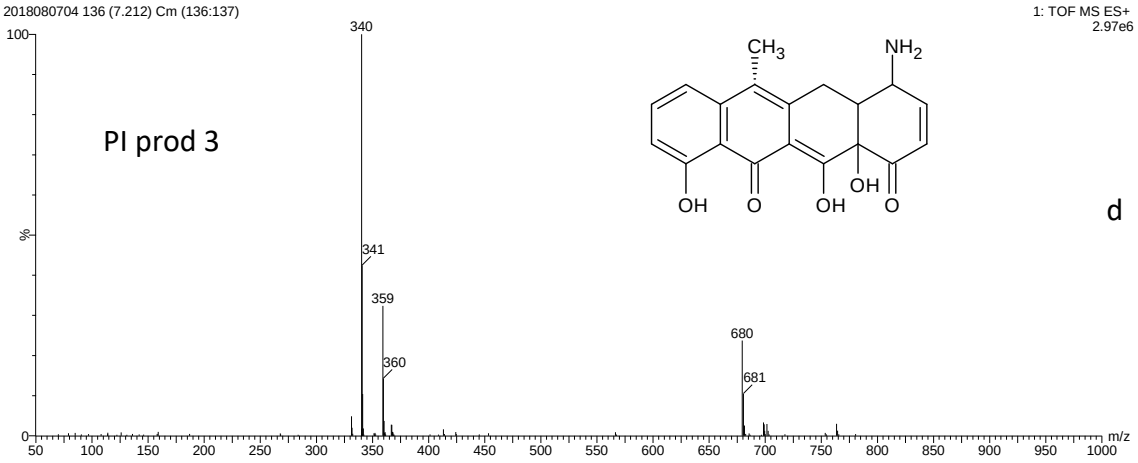

1012

1013

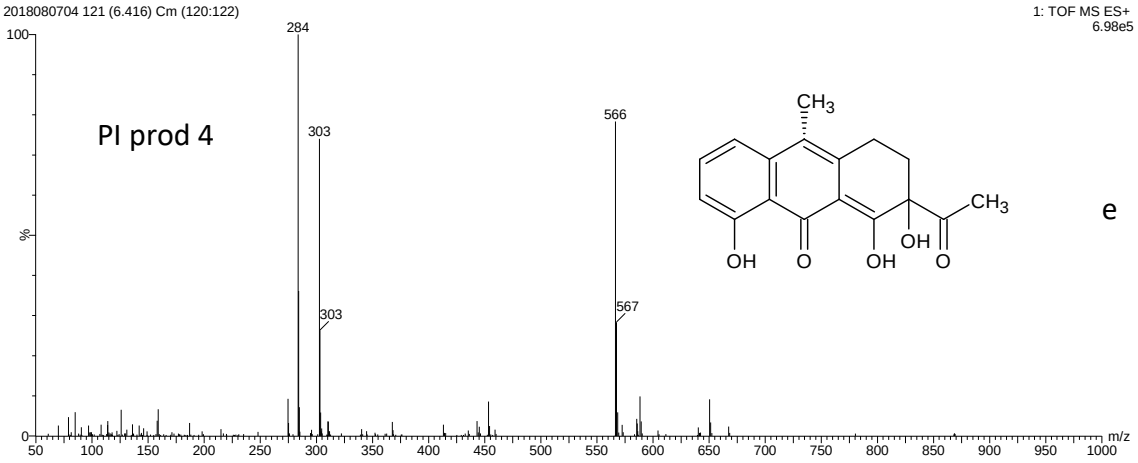

1014

1015

1016

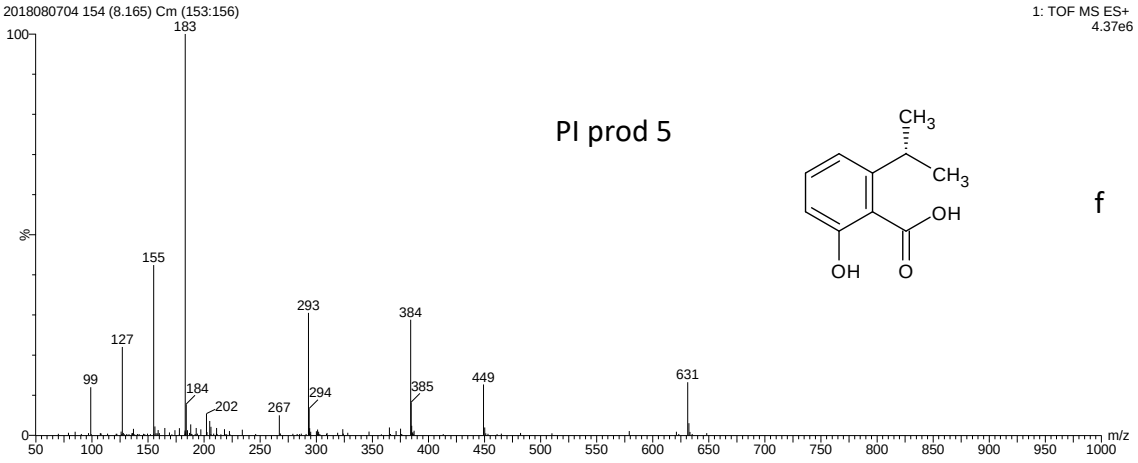

1017

1018

1019

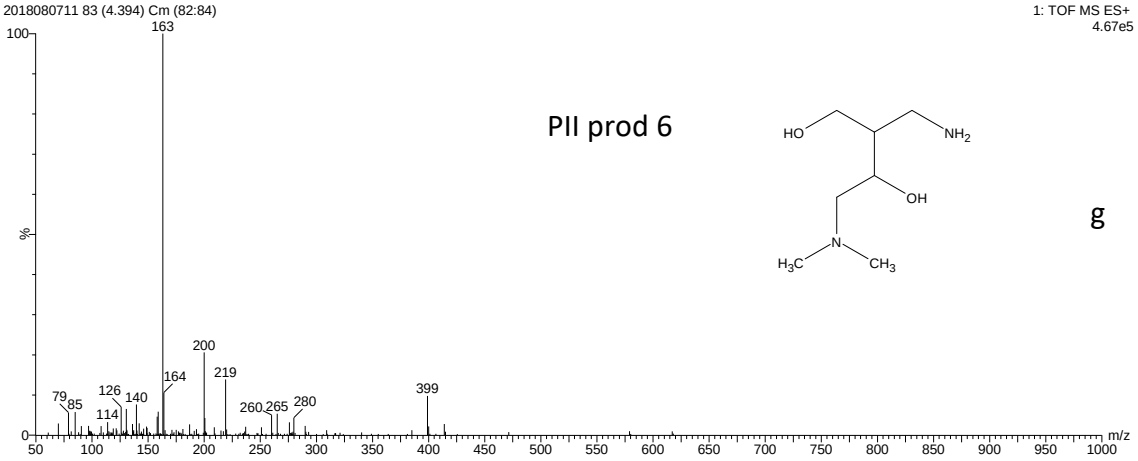

1020

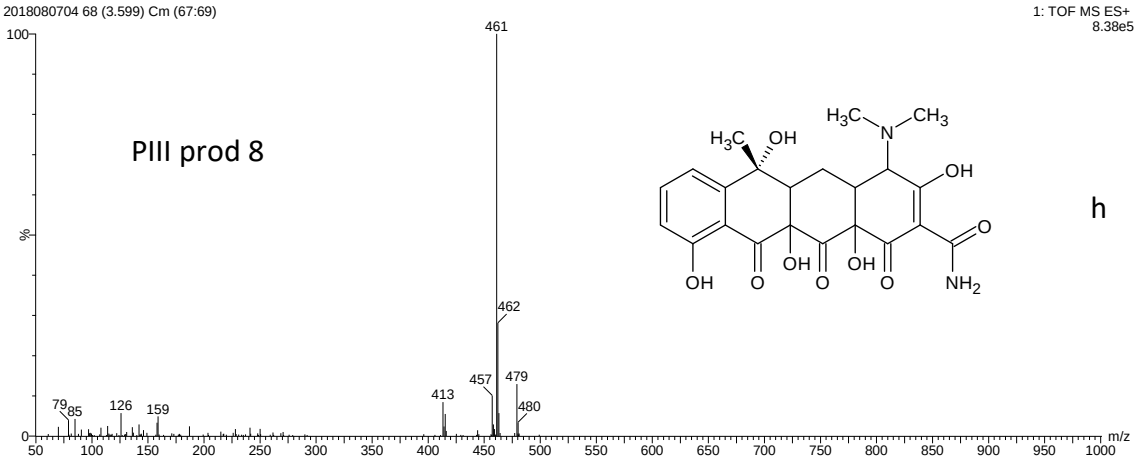

1021

1022

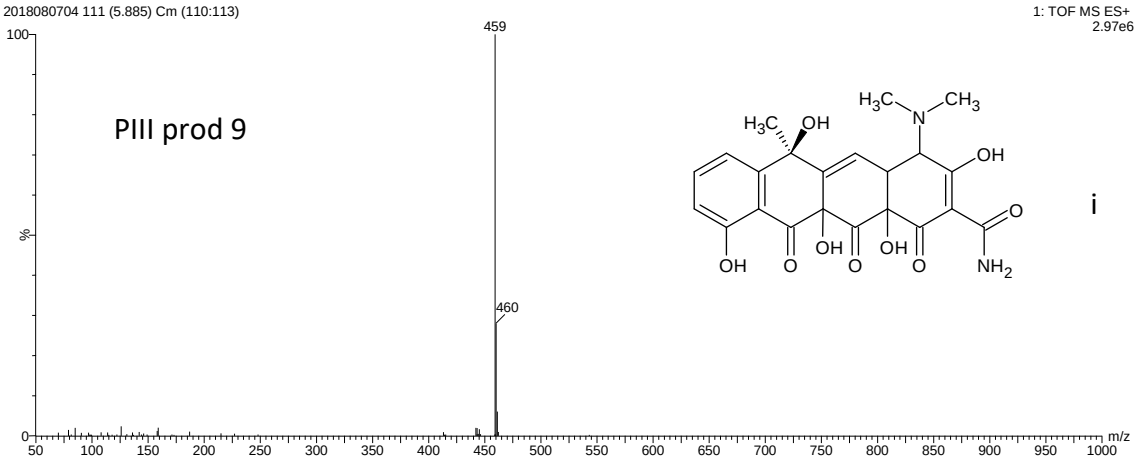

1023

Fig. ~~S4~~ S7 a-i. ESI-MS spectra of hypothesised tetracycline degradation products. In all cases the most intense signal represents the protonated molecular ion $[MH]^{+\cdot}$ for the compound suggested. Other peaks in the spectra may represent adduct ions, multimers, or other moieties originating from the chromatographic process.

Table S1 Composition of the BG11 growth medium

	Concentration (mg L^{-1})
$NaNO_3$	1500
K_2HPO_4	40
$MgSO_4 \cdot 7H_2O$	75
$CaCl_2 \cdot 2H_2O$	36
Citric acid	6
Ferric ammonium citrate	6
Na_2EDTA	1
Na_2CO_3	20
H_3BO_3	2.86
$MnCl_2 \cdot 4H_2O$	1.81
$ZnSO_4 \cdot 7H_2O$	0.22
$Na_2MoO_4 \cdot 2H_2O$	0.39
$CuSO_4 \cdot 5H_2O$	0.08
$Co(NO_3)_2 \cdot 6H_2O$	0.05

Table S2 Pseudo-first-order kinetic model fitting results of different removal pathways

Different removal pathways	Initial tetracycline concentration (mg L^{-1})	k value	R^2
Hydrolysis	50	$(6.9 \pm 0.6) \times 10^{-3}$	0.94
Photolysis	50	$(2.9 \pm 0.7) \times 10^{-2}$	0.90
Adsorption by *M. aeruginosa*	50	$(6.6 \pm 0.7) \times 10^{-1}$	0.98
Desorption by *M. aeruginosa*	50	$(2.3 \pm 0.0) \times 10^{-1}$	0.97
Adsorption by *C. pyrenoidosa*	50	$(3.7 \pm 0.8) \times 10^{-1}$	0.90
Desorption by *C. pyrenoidosa*	50	$(7.1 \pm 0.8) \times 10^{-3}$	0.92
Accumulation by *M. aeruginosa* (uptake)	50	$(1.9 \pm 0.3) \times 10^{-1}$	0.93
Accumulation by *M. aeruginosa* (decline)	50	$(1.2 \pm 0.1) \times 10^{-2}$	0.92
Accumulation by *C. pyrenoidosa* (uptake)	50	$(1.2 \pm 0.1) \times 10^{-1}$	0.96
Accumulation by *C. pyrenoidosa* (decline)	50	$(1.1 \pm 0.2) \times 10^{-2}$	0.90